
Contextual Explanation Networks

Maruan Al-Shedivat
Carnegie Mellon University
alshedivat@cs.cmu.edu

Avinava Dubey
Carnegie Mellon University
akdubey@cs.cmu.edu

Eric P. Xing
Carnegie Mellon University
epxing@cs.cmu.edu

Abstract

We introduce *contextual explanation networks (CENs)*—a class of models that learn to predict by generating and leveraging intermediate explanations. CENs combine deep networks with context-specific probabilistic models and construct explanations in the form of locally-correct hypotheses. Contrary to the existing *post-hoc* model-explanation tools, CENs learn to predict and to explain jointly. Our approach offers two major advantages: (i) for each prediction, valid instance-specific explanations are generated with no computational overhead and (ii) prediction via explanation acts as a regularization and boosts performance in low-resource settings. We prove that local approximations to the decision boundary of our networks are consistent with the generated explanations. Our results on image and text classification and survival analysis tasks demonstrate that CENs can easily match or outperform the state-of-the-art while offering additional insights behind each prediction, valuable for decision support.

1 Introduction

The recent empirical success of predictive algorithms promises to have a profound impact on shaping entire industries, from science [1] to healthcare [2], to public transportation [3]. The main drivers behind the success are the rapid growth of ubiquitous data and the algorithms and models that utilize such data efficiently. The top-performing methods are often based on minimal assumptions and are designed to learn complicated relationships directly from the data. This comes at a cost of interpretability—humans can no longer understand and trust the reasoning behind a particular decision of a complex algorithm. While the high performance often supports the belief in predictive capabilities of a system, perturbation analysis reveals that black-box models can be easily broken in an unintuitive and unexpected manner [4]. Therefore, for a machine learning system to be used in a social context (e.g., in healthcare) it is imperative to provide a sound reasoning for each decision.

Restricting the class of models to only *human-intelligible* [5] (e.g., generalized linear [6] and additive [7] models, decision trees, etc.) is a potential remedy, but often is too limiting in modern practical settings. Alternatively, one may fit a complex model and explain its predictions *post-hoc*, e.g., by searching for a simple local approximation of the decision boundary [8], or by inspecting the directions in the input space [9] that affect the prediction the most. While such approaches achieve their goal, the explanations are generated *a posteriori*, require additional computation per data instance, and, most importantly, are never the basis for the predictions made in the first place.

The explanation is a fundamental part of the human learning and decision process [10]. Inspired by this fact, we introduce *contextual explanation networks (CENs)*—a class of probabilistic models that learn to predict by constructing explanations. The key idea behind CENs is to combine deep networks with simple probabilistic graphical models that encode the prior knowledge. First, we note that modern datasets are often comprised of various representations, some of which are high-level and human-interpretable (e.g., categorical features), while many are low-level or unstructured (e.g., text, image pixels, sensory inputs). We define the *explanation* as a probabilistic model on the high-level features. Second, to account for the information available in the low-level representations,

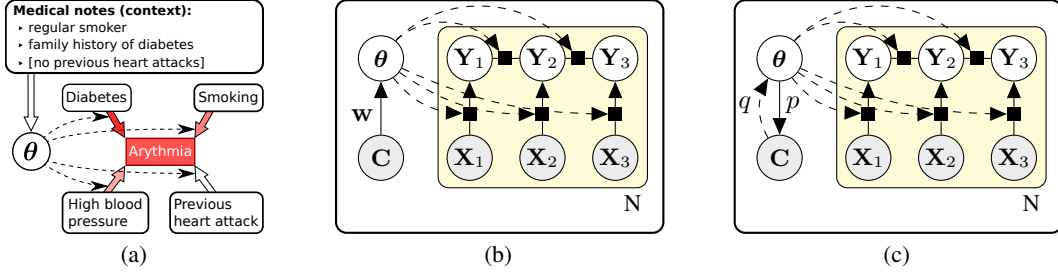


Figure 1: (a) An illustration of a contextual hypothesis for arrhythmia risk diagnosis. Shades of red denote the strength of association between the variables. (b) A graphical model for CEN with context encoder and CRF-based explanations. The model is parameterized by w . (c) A graphical model for CEN with context autoencoding via the inference network, $q_w(\theta | C)$, generator network, $p_u(C | \theta)$, and CRF-based explanations.

CENs use them as a *context* and require explanations to be context-specific [cf. context-specific PGM, 11, Ch. 5.3]. In particular, given a low-level representation of a data point (text, image, time series, etc.), we use a deep network designed for learning from such data modality to produce a *contextual hypothesis*, i.e., a probabilistic model that is applicable within the given context. For prediction, we apply the obtained hypothesis to the corresponding high-level features of the data instance. Importantly, the explanation mechanism is an integral part of CEN, and our models are trained to predict and to explain jointly.

A motivating example. Consider a CEN for diagnosing the risk of developing heart arrhythmia (Figure 1a). The causes of the condition are quite diverse, ranging from smoking and diabetes to an injury from previous heart attacks, and may carry different effects on the risk of arrhythmia in different contexts. Assume that the data for each patient consists of medical notes in the form of raw text (which is used as the *context*) and a number of specific attributes (such as high blood pressure, diabetes, smoking, etc.). Further, assume that we have access to a parametric class of expert-designed models that relate the attributes to the condition. The CEN maps the medical notes to the parameters of the model class to produce a *context-specific hypothesis*, which is further used to make a prediction.

In the sequel, we formalize these intuitions and refer to this toy example in our discussion to illustrate different aspects of the framework. The main contributions of the paper are as follows:

- We formally define CENs as a class of probabilistic models, consider special cases (e.g., mixture of experts [12]), and derive learning and inference algorithms for simple and structured outputs.
- We prove that explanations generated by CENs are consistent with the ones produced *post-hoc* via local approximations [8]. We also show that, in practice, while both methods generate explanations that are virtually identical, CENs construct them orders of magnitude faster.
- We implement CENs by extending a number of established domain-specific deep architectures for image and text data and design new architectures for survival analysis. Experimentally, we demonstrate the value of learning with explanations for prediction and model diagnostics.

2 Methods

We consider the problem of learning from a collection of data where each instance is represented by three random variables: *the context*, $C \in \mathcal{C}$, and *the attributes*, $X \in \mathcal{X}$, and *the targets*, $Y \in \mathcal{Y}$. The goal is to learn a model, $p_w(Y | X, C)$, parametrized by w that can predict Y from X and C . We define contextual explanation networks as models that assume the following form of the generative process and the predictive distribution (an example graphical model for CEN is given in Figure 1b):

$$Y \sim p(Y | X, \theta), \quad \theta \sim p_w(\theta | C), \quad p_w(Y | X, C) = \int p(Y | X, \theta) p_w(\theta | C) d\theta \quad (1)$$

where $p(Y | X, \theta)$ is a context-specific model (or hypothesis), which is parametrized by θ and depends on the attributes but *not* on the context. We call such hypotheses *explanations*¹, since they explicitly relate interpretable variables, X , to the targets, Y . For example, when the targets are scalar and binary, explanations may take the form of logistic regression; when the targets are more complex, dependencies between the components of Y can be modeled by a conditional random field [13].

¹When referring to $p(Y | X, \theta)$, we use the terms *hypothesis* and *explanation* interchangeably.

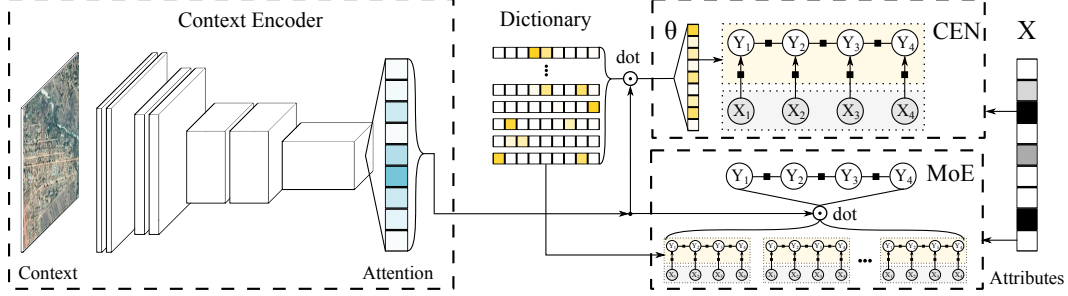


Figure 2: An example of CEN architecture. The context is represented by an image and transformed by a convnet encoder into an attention vector, which is used to construct a contextual hypothesis from a dictionary of sparse atoms. MoE uses a similar attention mechanism but for combining predictions of each model in the dictionary.

CENs assume that each explanation is context-specific: $p_w(\theta | \mathbf{C})$ defines a conditional probability of a hypothesis θ being valid in the context \mathbf{C} . To make a prediction, we marginalize out θ 's; to interpret a prediction, $\mathbf{Y} = \mathbf{y}$, for a given data instance, (\mathbf{x}, \mathbf{c}) , we infer the posterior, $p_w(\theta | \mathbf{Y} = \mathbf{y}, \mathbf{x}, \mathbf{c})$. The main advantage of this approach is that it allows modeling conditional probabilities, $p_w(\theta | \mathbf{C})$, in a black-box fashion while keeping the class of explanations, $p(\mathbf{Y} | \mathbf{X}, \theta)$, simple and interpretable. For instance, when the context is given as raw text, we could choose $p_w(\theta | \mathbf{C})$ to be represented with a recurrent neural network, while $p(\mathbf{Y} | \mathbf{X}, \theta)$ could be in the generalized linear class.

We discuss implications of the assumptions made by (1) in Appendix A. Here, we move on to describing a number of practical choices for $p_w(\theta | \mathbf{C})$ and learning and inference for those.

2.1 Contextual Explanation Networks

As a practical implementation of CEN, we represent $p_w(\theta | \mathbf{C})$ with a neural network that encodes the context into the parameter space of explanations. There are multiple ways to construct an encoder, which we consider below.

Deterministic Encoding. Consider $p_w(\theta | \mathbf{C}) := \delta(\phi_w(\mathbf{C}), \theta)$, where $\delta(\cdot, \cdot)$ is a delta-function. Collapsing the conditional distribution to a delta-function makes θ depend deterministically on \mathbf{C} and results into the following tractable conditional log-likelihood:

$$\log p(\mathbf{y}_i | \mathbf{x}_i, \mathbf{c}_i; \mathbf{w}) = \log \int p(\mathbf{y}_i | \mathbf{x}_i, \theta) \delta(\phi_w(\mathbf{c}_i), \theta) d\theta = \log p(\mathbf{y}_i | \mathbf{x}_i, \theta_i = \phi_w(\mathbf{c}_i)) \quad (2)$$

The conditional log-likelihood of each data point is local and determined by the corresponding explanation, $\theta_i = \phi_w(\mathbf{c}_i)$. Since $p_w(\theta_i | \mathbf{y}_i, \mathbf{x}_i, \mathbf{c}_i) \propto p(\mathbf{y}_i | \mathbf{x}_i, \theta_i) \delta(\phi_w(\mathbf{c}_i), \theta_i)$, the posterior also collapses to $\theta_i^* = \phi_w(\mathbf{c}_i)$, and hence the inference is done via a single forward pass.

Constrained Deterministic Maps. The downside of deterministic encoding is the lack of constraints on the generated explanations. There are multiple reasons why this might be an issue: (i) when the context encoder is unrestricted, it might generate unstable, overfitted local models, (ii) explanations are not guaranteed to be human-interpretable *per se*, and often require imposing additional constraints, such as sparsity, and (iii) when we want to reason about the patterns in the data as a whole, local explanations are not enough. To address these issues, we constrain the space of explanations by introducing a *global dictionary*, $\mathbf{D} := \{\theta_k\}_{k=1}^K$, where each atom of the dictionary, θ_k , is required to be sparse. The encoder generates context-specific explanations using *soft attention* over the dictionary (Figure 2), i.e., each local model becomes a convex combination of the sparse atoms:

$$\phi_{w, \mathbf{D}}(\mathbf{c}) = \sum_{k=1}^K p_w(k | \mathbf{c}) \theta_k = \alpha_w(\mathbf{c})^\top \mathbf{D}, \quad \sum_{k=1}^K \alpha_w^{(k)}(\mathbf{c}) = 1, \quad \forall k : \alpha_w^{(k)}(\mathbf{c}) \geq 0, \quad (3)$$

where $\alpha_w(\mathbf{c})$ is the context-specific attention over the dictionary. The model is trained by learning both the dictionary, \mathbf{D} , and the weights of the attention-based encoder, \mathbf{w} . The log-likelihood has the same form as given in (2), and both learning and inference are done via a single forward pass.

Mixtures of Experts. So far, we represented $p_w(\theta | \mathbf{C})$ by a delta-function centered around the output of an encoder. It is natural to extend $p_w(\theta | \mathbf{C})$ to a mixture of such delta-distributions, in which case CENs recover the well known class of models called *mixtures of experts (MoE)* [12]. In

particular, let $\mathbf{D} := \{\boldsymbol{\theta}_k\}_{k=1}^K$ be now a dictionary of experts, and define the encoder distribution as $p_{\mathbf{w},\mathbf{D}}(\boldsymbol{\theta} \mid \mathbf{C}) = \sum_{k=1}^K p_{\mathbf{w}}(k \mid \mathbf{C}) \delta(\boldsymbol{\theta}, \boldsymbol{\theta}_k)$. The log-likelihood in such case is the same as for MoE:

$$\log p_{\mathbf{w},\mathbf{D}}(\mathbf{y}_i \mid \mathbf{x}_i, \mathbf{c}_i) = \log \int p(\mathbf{y}_i \mid \mathbf{x}_i, \boldsymbol{\theta}) p_{\mathbf{w},\mathbf{D}}(\boldsymbol{\theta} \mid \mathbf{c}_i) d\boldsymbol{\theta} = \log \sum_{k=1}^K p_{\mathbf{w}}(k \mid \mathbf{c}_i) p(\mathbf{y}_i \mid \mathbf{x}_i, \boldsymbol{\theta}_k) \quad (4)$$

Note that $p_{\mathbf{w}}(k \mid \mathbf{C})$ is also represented as soft attention over the dictionary, \mathbf{D} , which is now used for combining predictions of each expert, $\boldsymbol{\theta}_k$, for a given context, \mathbf{C} , instead of constructing a single context-specific hypothesis. Learning is done by either directly optimizing the log-likelihood (4) or via EM [12]. To infer an explanation for a given context, we compute the posterior (see Appendix C).

Contextual Variational Autoencoders. Modeling $p(\mathbf{Y} \mid \mathbf{X}, \mathbf{C})$ in the form of (1) avoids representing the joint distribution, $p(\boldsymbol{\theta}, \mathbf{C})$, which is a good decision when the data is abundant. However, incorporating a generative model of the context has a few benefits: (i) better regularization in low-resource settings, and (ii) a coherent Bayesian framework that allows imposing additional priors on the parameter space of explanations. We further extend our framework by additionally modeling the distribution over the contexts via a decoder network. In particular, we build a variational autoencoder (VAE) [14, 15, 16] whose latent representations are explanations (Figure 1c). The generative process and the evidence lower bound (ELBO) for contextual VAEs are as follows:

$$\begin{aligned} \boldsymbol{\theta} &\sim p_{\alpha}(\boldsymbol{\theta}), \mathbf{C} \sim p_{\mathbf{u}}(\mathbf{C} \mid \boldsymbol{\theta}), \mathbf{Y} \sim p(\mathbf{Y} \mid \mathbf{X}, \boldsymbol{\theta}), \\ \log p(\mathbf{Y}, \mathbf{C} \mid \mathbf{X}) &\geq \mathbb{E}_{q_{\mathbf{w}}(\boldsymbol{\theta} \mid \mathbf{C})} [\log p(\mathbf{Y}, \mathbf{C} \mid \mathbf{X}, \boldsymbol{\theta})] - \text{KL}(q_{\mathbf{w}}(\boldsymbol{\theta} \mid \mathbf{C}) \parallel p(\boldsymbol{\theta})), \end{aligned} \quad (5)$$

where $p(\mathbf{Y}, \mathbf{C} \mid \mathbf{X}, \boldsymbol{\theta}) = p(\mathbf{Y} \mid \mathbf{X}, \boldsymbol{\theta}) p_{\mathbf{u}}(\mathbf{C} \mid \boldsymbol{\theta})$, and $p(\mathbf{Y} \mid \mathbf{X}, \boldsymbol{\theta})$ is the contextual explanation, and $q_{\mathbf{w}}(\boldsymbol{\theta} \mid \mathbf{C})$ and $p_{\mathbf{u}}(\mathbf{C} \mid \boldsymbol{\theta})$ the encoder and decoder, respectively. Note that the encoder, $q_{\mathbf{w}}(\boldsymbol{\theta} \mid \mathbf{C})$, can take the classical form of a Gaussian distribution with the location and scale parameterized by neural networks [15]. We consider encoders that make use of a global learnable dictionary, \mathbf{D} , and represent $q_{\mathbf{w}}(\boldsymbol{\theta} \mid \mathbf{C})$ in the form of Logistic Normal distribution over the simplex spanned by the atoms of \mathbf{D} . For the prior, $p(\boldsymbol{\theta})$, we use a Dirichlet distribution with parameters $\alpha_k < 1$ to induce sharp attention. Detailed derivations of the objective, learning, inference, and reparametrization for contextual VAEs are given in Appendix D.

2.2 CEN-generated vs. *post-hoc* Explanations

In this section, we analyze the relationship between CEN-generated and *post-hoc* explanations. If we regard CEN as a black-box function that takes (\mathbf{x}, \mathbf{c}) as input and outputs $f(\mathbf{x}, \mathbf{c}) := p(\mathbf{Y} \mid \mathbf{X} = \mathbf{x}, \mathbf{C} = \mathbf{c})$, we can use the LIME framework [8] and construct a local approximation of its decision boundary in the neighborhood of (\mathbf{x}, \mathbf{c}) in a *post-hoc* manner by solving the following optimization problem:

$$\hat{\boldsymbol{\theta}} = \underset{\boldsymbol{\theta}}{\text{argmin}} \mathcal{L}(f, \boldsymbol{\theta}, \pi_{\mathbf{x},\mathbf{c}}) + \Omega(\boldsymbol{\theta}), \quad (6)$$

where $\mathcal{L}(f, \boldsymbol{\theta}, \pi_{\mathbf{x},\mathbf{c}})$ measures the quality of $p(\mathbf{Y} \mid \mathbf{X}, \boldsymbol{\theta})$ as an approximation to f in the neighborhood of (\mathbf{x}, \mathbf{c}) , and $\Omega(\boldsymbol{\theta})$ is a regularizer that ensures interpretability of $\boldsymbol{\theta}$. The neighborhood of (\mathbf{x}, \mathbf{c}) is defined by a distribution $\pi_{\mathbf{x},\mathbf{c}}$ concentrated around the point of interest. The question we ask:

How does the local approximation, $\hat{\boldsymbol{\theta}}$, relate to the actual explanation, $\boldsymbol{\theta}^$, constructed by CEN in the first place to make a prediction?*

For the case of binary² classification, it turns out that when the context encoder is deterministic and the space of explanations is *linear*, local approximations, $\hat{\boldsymbol{\theta}}$, obtained by solving (6) recover the original hypotheses, $\boldsymbol{\theta}^*$, used for prediction. Formally, our result is stated in the following theorem.

Theorem 1. *Let the explanations and the local approximations be in the class of linear models, $p(Y = 1 \mid \mathbf{x}, \boldsymbol{\theta}) \propto \exp\{\mathbf{x}^\top \boldsymbol{\theta}\}$. Further, let the encoder be L -Lipschitz and pick a sampling distribution, $\pi_{\mathbf{x},\mathbf{c}}$, that concentrates around the point (\mathbf{x}, \mathbf{c}) , such that $p_{\pi_{\mathbf{x},\mathbf{c}}}(\|\mathbf{z}' - \mathbf{z}\| > t) < \varepsilon(t)$, where $\mathbf{z} := (\mathbf{x}, \mathbf{c})$ and $\varepsilon(t) \rightarrow 0$ as $t \rightarrow \infty$. Then, if the loss function is defined as*

$$\mathcal{L} = \frac{1}{K} \sum_{k=1}^K (\text{logit } p(Y = 1 \mid \mathbf{x}_k, \mathbf{c}_k) - \text{logit } p(Y = 1 \mid \mathbf{x}_k, \boldsymbol{\theta}))^2, (\mathbf{x}_k, \mathbf{c}_k) \sim \pi_{\mathbf{x},\mathbf{c}}, \quad (7)$$

the solution of (6) concentrates around $\boldsymbol{\theta}^$ as $\mathbb{P}_{\pi_{\mathbf{x},\mathbf{c}}}(\|\hat{\boldsymbol{\theta}} - \boldsymbol{\theta}^*\| > t) \leq \delta_{K,L}(t)$, for $\delta_{K,L} \xrightarrow[t \rightarrow \infty]{} 0$.*

²Analysis of the multi-class case can be reduced to the binary in the one-vs-all fashion.

By sampling from a distribution sharply concentrated around (\mathbf{x}, \mathbf{c}) , we ensure that $\hat{\theta}$ will recover θ^* with high probability. This result establishes an equivalence between the explanations generated by CENs and those generated by LIME *post-hoc*. The proof of the result is given in Appendix B.

2.3 Structured Explanations

We have shown that CEN-generated and *post-hoc* explanations turn out to be equivalent in the case of simple classification (i.e., when \mathbf{Y} is scalar). However, when \mathbf{Y} is structured (e.g., as a sequence), constructing coherent local approximation in a *post-hoc* manner is non-trivial. At the same time, CENs naturally let us represent $p(\mathbf{Y} | \mathbf{X}, \theta)$ using arbitrary graphical models. In this paper, we consider sequentially structured outputs and construct CENs with CRF-based explanations which we further apply to solve the survival analysis task, re-formulated as a structured prediction problem [17]. The general setup is as follows. Again, the data instances consist of contexts, attributes, and targets, $(\mathbf{C}, \mathbf{X}, \mathbf{Y})$, where now targets are sequences of m binary variables, $\mathbf{Y} := (y_1, \dots, y_m)$, that indicate occurrence of an event (e.g., death of a patient): if the event occurred at time $t \in [t_i, t_{i+1})$, then $y_j = 0, \forall j \leq i$ and $y_k = 1, \forall k > i$. Note that here, only $m + 1$ binary sequences are valid, i.e., assigned non-zero probability by the model. The CRF-based CEN is defined as follows:

$$\begin{aligned} \theta_t &\sim p_w(\theta | \mathbf{C}), t \in \{1, \dots, m\}, \quad \mathbf{Y} \sim p(\mathbf{Y} | \mathbf{X}, \theta_{1:m}), \\ p(\mathbf{Y} = (y_1, y_2, \dots, y_m) | \mathbf{x}, \theta_{1:m}) &\propto \exp \left\{ \sum_{i=1}^m y_i (\mathbf{x}^\top \theta_i) + \omega(y_i, y_{i+1}) \right\}. \end{aligned} \quad (8)$$

Here, the potentials between the attributes, \mathbf{x} , and the targets, $y_{1:m}$, are linear, parameterized by $\theta_{1:m}$; the pairwise potentials between targets, $\omega(y_i, y_{i+1})$, ensure that configurations $(y_i, y_{i+1}) = (1, 0)$ are improbable (i.e., $\omega(1, 0) = -\infty$). Following Chun-Nam et al. [17], we derive a tractable conditional log-likelihood in Appendix E. For $p_w(\theta | \mathbf{C})$, we chose to use a deterministic encoder with a global learnable dictionary. Learning and inference are done as described in the previous section.

3 Related work

As we have shown, CEN is a way to combine deep networks with structured probabilistic models. The idea of combining such models has been explored extensively; to mention a few, recent papers include work on structured prediction [e.g. 18, 19, 20], kernel learning [e.g., 21, 22], and state-space modeling [e.g., 23, 24]. The key difference between CENs and the previous art is that the latter proposed to directly integrate neural networks *into* the graphical models as components (e.g., neural potential functions). While flexible, the resulting *deep graphical models* could no longer be clearly interpreted in terms of crisp relationships between specific variables. The idea of generating parameters of deep network by another network is related and has been considered for zero-shot learning [25]. Other approaches to model interpretability, such as feature selection [26] and example-based model criticism [27, 28], are different but complementary to our explanation networks. Finally, we point out that our framework encompasses the class of so-called *personalized* or *instance-specific* models that learn to partition the space of inputs and fit local sub-models [e.g., 29].

4 Experiments

In this section, we proceed with an experimental evaluation of CENs. In particular, we consider applications that involve different data modalities of the context: image, text, and time series. In each case, CENs are based on deep architectures designed for learning from a given type of context; for the explanations, we use either a logistic regression (LR) or a conditional random field (CRF) [13]. We conduct experiments to verify the following statements:

- (i) CENs are able to match or surpass the performance of their vanilla deep network counterparts. Jointly learning to predict and to explain acts as a regularization and further boosts performance, especially in the small training data scenarios.
- (ii) Explanations generated by CENs are close to the ones generated *post-hoc* by LIME [8] not only in theory but also in practice. This means that CEN-generated explanations inherit the interpretability of LIME while eliminating the post-processing computation.
- (iii) Performance of CEN depends on how predictive the high-level features are of the targets, while LIME can overfit the decision boundary and hence lead to erroneous interpretations.

MNIST		CIFAR10		IMDB		Satellite		
Model	Err (%)	Model	Err (%)	Model	Err (%)	Model	Acc (%)	AUC (%)
LR _{px1}	8.00	LR _{px1}	60.1	LR _{bow}	13.3	LR _{emb}	62.5	68.1
LR _{hog}	2.98	LR _{hog}	48.6	LR _{tpc}	17.1	LR _{att}	75.7	82.2
CNN	0.75	VGG	9.4	LSTM	13.2	MLP	77.4	78.7
MoE _{px1}	1.23	MoE _{px1}	13.0	MoE _{bow}	13.9	MoE	77.9	85.4
MoE _{hog}	1.10	MoE _{hog}	11.7	MoE _{tpc}	12.2	CEN	81.5	84.2
CEN _{px1}	0.76	CEN _{px1}	9.6	CEN _{bow}	* 6.9	VCEN	83.4	84.6
CEN _{hog}	0.73	CEN _{hog}	9.2	CEN _{tpc}	* 7.8			

* Best previous results for similar LSTMs: 8.1% (supervised) and 6.6% (semi-supervised) [30].

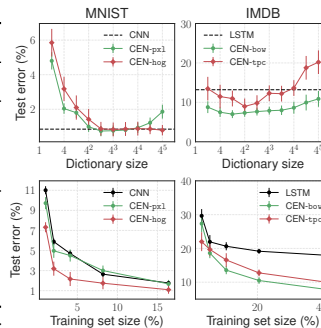


Table 1 & Figure 3: **Left:** Performance of the models on classification tasks (averaged over 5 runs; the std. are on the order of the least significant digit). The subscripts denote the features on which the linear models are built: pixels (px1), HOG (hog), bag-or-words (bow), topics (tpc), embeddings (emb), discrete attributes (att). **Right:** Results for vanilla deep nets and CENs for different dictionary sizes (upper) and train set sizes (lower).

4.1 Classification tasks

Classical datasets. We consider the two classical image datasets, MNIST³ and CIFAR10⁴, and a text dataset for sentiment classification of the IMDB reviews [31]. For MNIST and CIFAR: the images are used as context; to imitate high-level features, we use (a) the original images cubically downsampled to 20×20 pixels, gray-scaled and normalized, and (b) HOG descriptors [32]; a simple convnet (2 convolutions followed by a max pooling layer) for MNIST and the VGG-16 architecture [33] for CIFAR10 are used as baselines and also as the context encoders in CEN. For IMDB: the context is represented by sequences of words; for high-level features we use (a) the bag-of-words (BoW) representation and (b) a topic representation produced by a separately trained topic model; a bi-directional LSTM with pooling [30] is used as a baseline and context encoder.

Remote sensing. We also consider the problem of poverty prediction for household clusters in a developing country (Uganda) from satellite imagery and survey data. Each household cluster is represented by a collection of 400×400 satellite images and a vector of categorical features. The satellite images are considered as the context; 65 variables from living standards measurement survey (LSMS) are used as the high-level interpretable features (these data representations are *not* derivatives of each other). The task is binary classification of households in Uganda into poor and not poor. We closely follow the original study of Jean et al. [34] and use a pretrained VGG-F network for embedding the images into a 4096-dimensional space on top of which we build our contextual models. Note that this datasets is fairly small (642 points), and hence we keep the VGG-F frozen to avoid overfitting.

Models. For each task, we used linear regression and the vanilla deep networks as baselines. CENs used the baseline deep nets as context encoders and were of three types: (a) mixture of experts (MoE), (b) deterministic context encoding (CEN) and (c) variational context autoencoding (VCEN), all with the dictionary constraint and sparsity regularization (see Section 2.1). Additional details on the parametrization and training procedures are given in Appendix F.

Quantitative analysis. Performance of the models across different tasks is given in Table 1. In each task, CENs are trained to simultaneously generate predictions and construct explanations using a dictionary (the size varied from 2 to 1024, see Figure 3, upper panel) and are able to match or outperform the vanilla deep nets and linear models. On the image data, CENs with linear explanations on HOG descriptors give a slight improvement over the baseline performance. On the IMDB text data, CENs surpass the state of the art result for supervised classification attainable by the LSTM architectures [30]. When the models are trained on a subset of data (the size varied from 1% to 20% for MNIST and from 2% to 40% for IMDB), we notice that explanations play the role of a regularizer which strongly improves the sample complexity of our models (Figure 3, lower panel). This becomes even more evident from the results on the Satellite dataset that had only 500 training points. There, CEN, VCEN, and MoE models use satellite imagery as context and significantly improved upon the sparse linear models on the survey features (known as the gold standard in remote sensing techniques). Note that training an MLP on both encoded satellite images and survey features, while beneficial, does not come close to the result achieved by contextual explanation networks.

³<http://yann.lecun.com/exdb/mnist/>

⁴<http://www.cs.toronto.edu/~kriz/cifar.html>

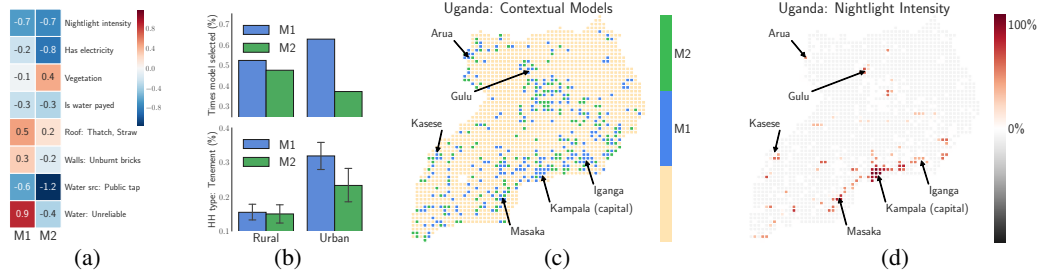


Figure 4: Qualitative results for the Satellite dataset: (a) Weights given to a subset of features by the two models (M1 and M2) discovered by CEN. (b) How frequently M1 and M2 are selected for areas marked rural or urban (top) and the average proportion of Tenement-type households in an urban/rural area for which M1 or M2 was selected. (c) M1 and M2 models selected for different areas on the Uganda map. M1 tends to be selected for more urbanized areas while M2 is picked for the rest. (d) Nightlight intensity of different areas of Uganda.

Qualitative analysis. To analyze CEN-generated explanations qualitatively, we focus on the poverty prediction task (see Appendix F for visualizations of the learned models for images and text). We discover that, after convergence, CENs tend to sharply select one of the two linear models (M1 and M2) for different household clusters in Uganda (Figure 4a). In the survey data, each household cluster is marked as either urban or rural; we notice that CEN tends to pick M1 for urban areas and M2 for rural⁵ (Figure 4b). Notice that the models weigh different categorical features, such as reliability of the water source or the proportion of houses with walls made of unburnt brick, quite differently. When visualized on the map, we see that CEN selects M1 more frequently around the major city areas, which also correlates with high nightlight intensity in those areas (Figures 4c-4d).

Comparison with LIME. While training models to jointly predict and explain is a powerful regularization mechanism, the primary use case for explanations themselves is model diagnostics. LIME [8] is positioned as a useful tool for the latter purpose. As we have shown in Section 2.2, under certain conditions, LIME applied to CEN recovers the original explanations with high probability (Theorem 1). We test this experimentally on the IMDB dataset and CEN_{low} model: First, we use a trained CEN model to generate linear explanations on the BoW features for a number of validation points. Then, we generate explanations using LIME by sampling 10k points in the neighborhood of each point⁶ and approximating the decision boundary. The relative L_1 -distance between the CEN- and LIME-generated explanations is $4.1 \pm 0.6\%$ indicating that the explanations are virtually identical. Further, we compare CEN and LIME in terms of the compute time overhead (Table 2): While CENs have a negligible overhead in training time compared to the vanilla deep nets, they generate explanations via a single forward pass and are orders of magnitude faster than LIME⁷.

Table 2: Compute time overhead.

Training time overhead		
Dataset	CEN	LIME [8]
IMDB	$1.8 \pm 0.5\%$	—
Satellite	$0.4 \pm 0.1\%$	—
Explanation generation time p/ instance		
Dataset	CEN	LIME [8]
IMDB	0.07 ± 0.03 ms	38 ± 5 ms
Satellite	0 ± 0.01 ms	22 ± 6 ms

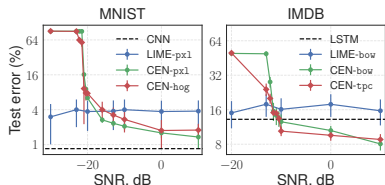


Figure 5: Test accuracy vs. the level of the noise added to the interpretable features.

accurately fit and “explain” the decision boundary of the deep network (Figure 5). This shows one of the main drawbacks of the *post-hoc* explanations: when constructed using poor or noisy features, they can overfit the decision boundary and produce explanations that are likely to be misleading.

Finally, we ask the question, *what happens if the high-level features used for model explanation were poorly correlated with the targets?* To test this, we add noise to the features, \mathbf{X} , but *not* to the context, \mathbf{C} , and train CEN (on \mathbf{C} and noisy \mathbf{X}) and a vanilla deep network (only on \mathbf{C}). To produce explanations for the latter, we fit LIME to predict outputs of the deep network from noisy \mathbf{X} . As more noise is added, CEN’s performance deteriorates. At the same time, regardless of the amount of added noise, LIME is able to more or less

⁵This turns out to be consistent the original study [34] which showed that convolutional networks were good at detecting infrastructure on satellite imagery.

⁶The sampling was done via 2% perturbation of the BoW features with Poisson noise.

⁷We measure only the time LIME takes to solve the optimization problem (6) to produce the approximation. Note that LIME additionally requires to sample model predictions in the neighborhood of each point of interest, i.e., it needs to compute on the order of a few thousand forward passes atop of the optimization overhead.

Table 3: Performance of the classical Cox and Aalen models, CRF-based models, and CEMs that use LSTM or MLP for context embedding and CRF for explanations. The numbers are averages from 5-fold cross-validation; the std. are on the order of the least significant digit. @K denotes the temporal quantile, i.e., the time point such that K% of the patients in the data have died or were censored before that point.

SUPPORT2					PhysioNet Challenge 2012				
Model	Acc@25	Acc@50	Acc@75	RAE	Model	Acc@25	Acc@50	Acc@75	RAE
Cox	82.5	83.3	18.2	0.77	Cox	93.0	69.6	49.1	0.24
Aalen	86.7	78.4	49.5	0.65	Aalen	93.3	78.7	57.1	0.31
CRF	81.6	99.0	84.7	0.50	CRF	93.2	85.1	65.6	0.14
MLP-CRF	87.2	99.2	85.8	0.49	LSTM-CRF	93.9	86.3	68.1	0.11
MLP-CEN	90.4	99.2	87.1	0.44	LSTM-CEN	94.8	87.5	70.1	0.09

4.2 Survival Analysis

Finally, we apply CENs to survival analysis of the intense care unit (ICU) patients. In survival analysis, the goal is to learn a predictor for the time of occurrence of an event (in this case, the death of a patient) as well as be able to assess the risk (or hazard) of the occurrence. The classical models for this task are the Aalen’s additive model [35] and the Cox proportional hazard model [36], which linearly regress attributes of a particular patient, \mathbf{X} , to the hazard function. Recently, it has been shown that CRF is more suitable, shows better performance in certain cases, and can be interpreted as a sequence of time-specific linear models [17]. Hence, as described in Section 4.2, we cast the survival analysis problem into structured prediction and use linear CRF-based explanations.

Datasets and metrics. We use two publicly available datasets for survival analysis of the ICU patients: (a) SUPPORT2⁸ (9105 patient records, 51 attributes), and (b) data from the PhysioNet 2012 challenge⁹ (each data instance is represented by a 48-hour irregularly sampled 37-dimensional time-series for 4000 patients). The data is used as follows:

- (a) We duplicate the attributes and assume that the context and the high-level features are the same (i.e., $\mathbf{C} \equiv \mathbf{X}$); the context is encoded by a multi-layer perceptron (MLP).
- (b) The full time-series are used as the context; for high-level features, we take the values of the last available measurement for each variable in the time-series; LSTM is used for context encoding.

For metrics, we used accuracy of predicting survival of a patient at times that corresponded to 25%, 50%, and 75% population-level quantiles and the relative absolute error (RAE) measured as in [17].

Results. The results are given in Table 3. Our implementation of the CRF baseline reproduces (and even slightly improves) the performance reported by Chun-Nam et al. [17]. MLP-CRF and LSTM-CRF use hidden representations produced by the neural networks as CRF features. While improving performance, these models assign weights to features of the hidden neural representations and can no longer be interpreted in terms of the original variables. Using MLP and LSTM as context encoders, CENs are able to attain very competitive results while providing explanations for each risk prediction at each point in time.

5 Conclusion

In this paper, we have introduced contextual explanation networks (CENs)—models that learn to predict by constructing and applying simple context-specific hypotheses. We have formally defined CENs as a class of probabilistic models, considered a number of special cases (e.g., the mixture of experts), and derived learning and inference procedures within the encoder-decoder framework for simple and sequentially-structured outputs. Learning to predict and to explain jointly turned out to have a number of benefits, including strong regularization, consistency, and the ability to generate explanations with no computational overhead. As shown both theoretically and experimentally, under certain conditions, explanations generated by CENs are close or equivalent to those generated *post-hoc*. We believe that the proposed class of models may be quite useful not only for improving prediction capabilities, but also for model diagnostics, pattern discovery, and general data analysis, especially when machine learning is used for decision support in high-stakes applications.

⁸<http://biostat.mc.vanderbilt.edu/wiki/Main/DataSets>.

⁹<https://physionet.org/challenge/2012/>.

Acknowledgements

We thank Willie Neiswanger and Mrinmaya Sachan for many useful comments on an early draft of the paper, and Ahmed Hefny, Shashank J. Reddy, Bryon Aragam, and Russ Salakhutdinov for helpful discussions. We also thank Neal Jean for making available the code that helped us conduct experiments on the satellite imagery data. This work was supported by NIH R01GM114311 and AFRL/DARPA FA87501220324.

References

- [1] Yolanda Gil, Mark Greaves, James Hendler, and Haym Hirsh. “Amplify scientific discovery with artificial intelligence”. In: *Science* 346.6206 (2014), pp. 171–172.
- [2] Francis S Collins and Harold Varmus. “A new initiative on precision medicine”. In: *New England Journal of Medicine* 372.9 (2015), pp. 793–795.
- [3] Jesse Levinson et al. “Towards fully autonomous driving: Systems and algorithms”. In: *Intelligent Vehicles Symposium (IV), 2011 IEEE*. IEEE. 2011, pp. 163–168.
- [4] Christian Szegedy, Wojciech Zaremba, Ilya Sutskever, Joan Bruna, Dumitru Erhan, Ian Goodfellow, and Rob Fergus. “Intriguing properties of neural networks”. In: *arXiv preprint arXiv:1312.6199* (2013).
- [5] Rich Caruana et al. “Intelligible models for healthcare: Predicting pneumonia risk and hospital 30-day readmission”. In: *Proceedings of the 21th ACM SIGKDD International Conference on Knowledge Discovery and Data Mining*. ACM. 2015, pp. 1721–1730.
- [6] Peter McCullagh and John A Nelder. *Generalized linear models*. Vol. 37. CRC press, 1989.
- [7] Trevor J Hastie and Robert J Tibshirani. *Generalized additive models*. Vol. 43. CRC Press, 1990.
- [8] Marco Tulio Ribeiro, Sameer Singh, and Carlos Guestrin. “Why Should I Trust You?: Explaining the Predictions of Any Classifier”. In: *Proceedings of the 22nd ACM SIGKDD International Conference on Knowledge Discovery and Data Mining*. ACM. 2016, pp. 1135–1144.
- [9] David Baehrens, Timon Schroeter, Stefan Harmeling, Motoaki Kawanabe, Katja Hansen, and Klaus-Robert MÅžller. “How to explain individual classification decisions”. In: *Journal of Machine Learning Research* 11.Jun (2010), pp. 1803–1831.
- [10] Tania Lombrozo. “The structure and function of explanations”. In: *Trends in cognitive sciences* 10.10 (2006), pp. 464–470.
- [11] Daphne Koller and Nir Friedman. *Probabilistic Graphical Models: Principles and Techniques*. MIT press, 2009.
- [12] Robert A Jacobs, Michael I Jordan, Steven J Nowlan, and Geoffrey E Hinton. “Adaptive mixtures of local experts”. In: *Neural computation* 3.1 (1991), pp. 79–87.
- [13] John Lafferty, Andrew McCallum, Fernando Pereira, et al. “Conditional random fields: Probabilistic models for segmenting and labeling sequence data”. In: *Proceedings of the eighteenth international conference on machine learning, ICML*. Vol. 1. 2001, pp. 282–289.
- [14] Geoffrey E Hinton, Peter Dayan, Brendan J Frey, and Radford M Neal. “The “wake-sleep” algorithm for unsupervised neural networks”. In: *Science* 268.5214 (1995), p. 1158.
- [15] Diederik P Kingma and Max Welling. “Auto-encoding variational bayes”. In: *arXiv preprint arXiv:1312.6114* (2013).
- [16] Danilo Jimenez Rezende, Shakir Mohamed, and Daan Wierstra. “Stochastic Backpropagation and Approximate Inference in Deep Generative Models”. In: *Proceedings of The 31st International Conference on Machine Learning*. 2014, pp. 1278–1286.
- [17] J Yu Chun-Nam, Russell Greiner, Hsiu-Chin Lin, and Vickie Baracos. “Learning patient-specific cancer survival distributions as a sequence of dependent regressors”. In: *Advances in Neural Information Processing Systems*. 2011, pp. 1845–1853.
- [18] Ronan Collobert, Jason Weston, Léon Bottou, Michael Karlen, Koray Kavukcuoglu, and Pavel Kuksa. “Natural language processing (almost) from scratch”. In: *Journal of Machine Learning Research* 12.Aug (2011).
- [19] Max Jaderberg, Karen Simonyan, Andrea Vedaldi, and Andrew Zisserman. “Deep structured output learning for unconstrained text recognition”. In: *arXiv preprint arXiv:1412.5903* (2014).
- [20] David Belanger and Andrew McCallum. “Structured prediction energy networks”. In: *Proceedings of the International Conference on Machine Learning*. 2016.

- [21] Andrew Gordon Wilson, Zhiting Hu, Ruslan Salakhutdinov, and Eric P Xing. “Deep kernel learning”. In: *Proceedings of the 19th International Conference on Artificial Intelligence and Statistics*. 2016, pp. 370–378.
- [22] Maruan Al-Shedivat, Andrew Gordon Wilson, Yunus Saatchi, Zhiting Hu, and Eric P Xing. “Learning Scalable Deep Kernels with Recurrent Structure”. In: *arXiv preprint arXiv:1610.08936* (2016).
- [23] Rahul G Krishnan, Uri Shalit, and David Sontag. “Deep kalman filters”. In: *arXiv preprint arXiv:1511.05121* (2015).
- [24] Matthew Johnson, David K Duvenaud, Alex Wiltschko, Ryan P Adams, and Sandeep R Datta. “Composing graphical models with neural networks for structured representations and fast inference”. In: *Advances in Neural Information Processing Systems*. 2016, pp. 2946–2954.
- [25] Jimmy Lei Ba, Kevin Swersky, Sanja Fidler, and Ruslan Salakhutdinov. “Predicting deep zero-shot convolutional neural networks using textual descriptions”. In: *Proceedings of the IEEE International Conference on Computer Vision*. 2015, pp. 4247–4255.
- [26] Been Kim, Julie A Shah, and Finale Doshi-Velez. “Mind the gap: A generative approach to interpretable feature selection and extraction”. In: *Advances in Neural Information Processing Systems*. 2015, pp. 2260–2268.
- [27] Rich Caruana, Hooshang Kangarloo, JD Dionisio, Usha Sinha, and David Johnson. “Case-based explanation of non-case-based learning methods.” In: *Proceedings of the AMIA Symposium*. 1999, p. 212.
- [28] Been Kim, Oluwasanmi O Koyejo, and Rajiv Khanna. “Examples are not enough, learn to criticize! Criticism for Interpretability”. In: *Advances In Neural Information Processing Systems*. 2016, pp. 2280–2288.
- [29] Joseph Wang and Venkatesh Saligrama. “Local Supervised Learning through Space Partitioning”. In: *NIPS*. 2012.
- [30] Rie Johnson and Tong Zhang. “Supervised and Semi-Supervised Text Categorization using LSTM for Region Embeddings”. In: *Proceedings of The 33rd International Conference on Machine Learning*. 2016, pp. 526–534.
- [31] Andrew L Maas, Raymond E Daly, Peter T Pham, Dan Huang, Andrew Y Ng, and Christopher Potts. “Learning word vectors for sentiment analysis”. In: *Proceedings of the 49th Annual Meeting of the Association for Computational Linguistics: Human Language Technologies-Volume 1*. Association for Computational Linguistics. 2011, pp. 142–150.
- [32] Navneet Dalal and Bill Triggs. “Histograms of oriented gradients for human detection”. In: *Computer Vision and Pattern Recognition, 2005. CVPR 2005. IEEE Computer Society Conference on*. Vol. 1. IEEE. 2005, pp. 886–893.
- [33] Karen Simonyan and Andrew Zisserman. “Very deep convolutional networks for large-scale image recognition”. In: *arXiv preprint arXiv:1409.1556* (2014).
- [34] Neal Jean, Marshall Burke, Michael Xie, W Matthew Davis, David B Lobell, and Stefano Ermon. “Combining satellite imagery and machine learning to predict poverty”. In: *Science* 353.6301 (2016), pp. 790–794.
- [35] O.O. Aalen. “A linear regression model for the analysis of life time”. In: *Statistics in Medicine*, 8(8):907–925 (1989).
- [36] DR Cox. “Regression Models and Life-Tables”. In: *Journal of the Royal Statistical Society. Series B (Methodological)* (1972), pp. 187–220.

A Analysis of the assumptions made by CEN

As described in the main text, CENs represent the predictive distribution in the following form:

$$p(\mathbf{Y} | \mathbf{X}, \mathbf{C}) = \int p(\mathbf{Y} | \mathbf{X}, \boldsymbol{\theta}) p(\boldsymbol{\theta} | \mathbf{C}) d\boldsymbol{\theta}$$

and the assumed generative process behind the data is either:

- (CEN) $\mathbf{Y} \sim p(\mathbf{Y} | \mathbf{X}, \boldsymbol{\theta})$, $\boldsymbol{\theta} \sim p(\boldsymbol{\theta} | \mathbf{C})$ for the purely discriminative setting.
- (VCEN) $\mathbf{Y} \sim p(\mathbf{Y} | \mathbf{X}, \boldsymbol{\theta})$, $\boldsymbol{\theta} \sim p(\boldsymbol{\theta})$, $\mathbf{C} \sim p(\mathbf{C} | \boldsymbol{\theta})$ when we model the joint distribution of the explanations, $\boldsymbol{\theta}$, and contexts, \mathbf{C} , e.g., using encoder-decoder framework.

We would like to understand whether CEN, as defined above, can represent any conditional distribution, $p(\mathbf{Y} | \mathbf{X}, \mathbf{C})$, when the class of explanations is limited (e.g., to linear models), and, if not, what are the limitations?

Generally, CEN can be seen as a mixture of predictors. Such mixture models could be quite powerful as long as the mixing distribution, $p(\boldsymbol{\theta} | \mathbf{C})$, is rich enough. In fact, even a finite mixture exponential family regression models can approximate any smooth d -dimensional density at a rate $O(m^{-4/d})$ in the KL-distance [1]. This result suggests that representing the predictive distribution with contextual mixtures should not limit the representational power of the model. The two caveats are:

- (i) In practice, $p(\boldsymbol{\theta} | \mathbf{C})$ is limited, e.g., either deterministic encoding, a finite mixture, or a simple distribution parametrized by a deep network.
- (ii) The classical setting of predictive mixtures does not separate inputs into two subsets, (\mathbf{C}, \mathbf{X}) . We do this intentionally to produce hypotheses/explanations in terms of specific features that could be useful for interpretability or model diagnostics down the line. However, it could be the case that \mathbf{X} contains only some limited information about \mathbf{Y} , which could limit the predictive power of the full model.

We leave the point (ii) to future work. To address (i), we consider $p(\boldsymbol{\theta} | \mathbf{C})$ that fully factorizes over the dimensions of $\boldsymbol{\theta}$: $p(\boldsymbol{\theta} | \mathbf{C}) = \prod_j p(\theta_j | \mathbf{C})$, and assume that hypotheses, $p(\mathbf{Y} | \mathbf{X}, \boldsymbol{\theta})$, factorize according to some underlying graph, $\mathcal{G}_{\mathbf{Y}} = (\mathcal{V}_{\mathbf{Y}}, \mathcal{E}_{\mathbf{Y}})$. The following proposition shows that in such case $p(\mathbf{Y} | \mathbf{X}, \mathbf{C})$ inherits the factorization properties of the hypothesis class.

Proposition 1. *Let $p(\boldsymbol{\theta} | \mathbf{C}) := \prod_j p(\theta_j | \mathbf{C})$ and let $p(\mathbf{Y} | \mathbf{X}, \boldsymbol{\theta})$ factorize according to some graph $\mathcal{G}_{\mathbf{Y}} = (\mathcal{V}_{\mathbf{Y}}, \mathcal{E}_{\mathbf{Y}})$. Then, $p(\mathbf{Y} | \mathbf{X}, \mathbf{C})$ defined by CEN with $p(\boldsymbol{\theta} | \mathbf{C})$ encoder and $p(\mathbf{Y} | \mathbf{X}, \boldsymbol{\theta})$ explanations also factorizes according to \mathcal{G} .*

Proof. Assume that $p(\mathbf{Y} | \mathbf{X}, \boldsymbol{\theta})$ factorizes as $\prod_{\alpha \in \mathcal{V}_{\mathbf{Y}}} p(\mathbf{Y}_{\alpha} | \mathbf{Y}_{\text{MB}(\alpha)}, \mathbf{X}, \boldsymbol{\theta}_{\alpha})$, where α denotes subsets of the \mathbf{Y} variables and $\text{MB}(\alpha)$ stands for the corresponding Markov blankets. Using the definition of CEN, we have:

$$p(\mathbf{Y} | \mathbf{X}, \mathbf{C}) = \int p(\mathbf{Y} | \mathbf{X}, \boldsymbol{\theta}) p(\boldsymbol{\theta} | \mathbf{C}) d\boldsymbol{\theta} \quad (9)$$

$$= \int \prod_{\alpha \in \mathcal{V}_{\mathbf{Y}}} p(\mathbf{Y}_{\alpha} | \mathbf{Y}_{\text{MB}(\alpha)}, \mathbf{X}, \boldsymbol{\theta}_{\alpha}) \prod_j p(\theta_j | \mathbf{C}) d\boldsymbol{\theta} \quad (10)$$

$$= \prod_{\alpha \in \mathcal{V}_{\mathbf{Y}}} \left[\int p(\mathbf{Y}_{\alpha} | \mathbf{Y}_{\text{MB}(\alpha)}, \mathbf{X}, \boldsymbol{\theta}_{\alpha}) \prod_{j \in \alpha} p(\theta_j | \mathbf{C}) d\boldsymbol{\theta}_{\alpha} \right] \quad (11)$$

$$= \prod_{\alpha \in \mathcal{V}_{\mathbf{Y}}} p(\mathbf{Y}_{\alpha} | \mathbf{Y}_{\text{MB}(\alpha)}, \mathbf{X}, \mathbf{C}), \quad (12)$$

□

Remark 1. *All the encoding distributions, $p(\boldsymbol{\theta} | \mathbf{C})$, considered in the main text of the paper, including delta functions, their mixtures, and encoders parametrized by neural nets fully factorize over the dimensions of $\boldsymbol{\theta}$.*

Remark 2. *The proposition has no implications for the case of scalar targets, \mathbf{Y} . However, in case of structured prediction, regardless of how good the context encoder is, CEN will assume the same set of independencies as given by the class of hypotheses, $p(\mathbf{Y} | \mathbf{X}, \boldsymbol{\theta})$.*

B Approximating the Decision Boundary of CEN

Ribeiro et al. [2] proposed to construct approximations of the of the decision boundary of an arbitrary predictor, f , in the locality of a specified point, \mathbf{x} , by solving the following optimization problem:

$$\hat{g} = \operatorname{argmin}_{g \in G} \mathcal{L}(f, g, \pi_{\mathbf{x}}) + \Omega(g), \quad (13)$$

where $\mathcal{L}(f, g, \pi_{\mathbf{x}})$ measures the quality of g as an approximation to f in the neighborhood of \mathbf{x} defined by $\pi_{\mathbf{x}}$ and $\Omega(g)$ is a regularizer that is usually used to ensure human-interpretability of the selected local hypotheses (e.g., sparsity). Now, consider the case when f is defined by a CEN, instead of \mathbf{x} we have (\mathbf{c}, \mathbf{x}) , and the class of approximations, G , coincides with the class of explanations, and hence can be represented by $\boldsymbol{\theta}$. In this setting, we can pose the same problem as:

$$\hat{\boldsymbol{\theta}} = \operatorname{argmin}_{\boldsymbol{\theta}} \mathcal{L}(f, \boldsymbol{\theta}, \pi_{\mathbf{c}, \mathbf{x}}) + \Omega(\boldsymbol{\theta}) \quad (14)$$

Suppose that CEN produces $\boldsymbol{\theta}^*$ explanation for the context \mathbf{c} using a deterministic encoder, ϕ . The question is whether and under which conditions $\hat{\boldsymbol{\theta}}$ can recover $\boldsymbol{\theta}^*$. Theorem 1 answers the question in affirmative and provides a concentration result for the case when hypotheses are linear. Here, we prove Theorem 1 for a little more general class of log-linear explanations: $\operatorname{logit} p(Y = 1 | \mathbf{x}, \boldsymbol{\theta}) = \mathbf{a}(\mathbf{x})^\top \boldsymbol{\theta}$, where \mathbf{a} is a C -Lipschitz vector-valued function whose values have a zero-mean distribution when (\mathbf{x}, \mathbf{c}) are sampled from $\pi_{\mathbf{x}, \mathbf{c}}$ ¹⁰. For simplicity of the analysis, we consider binary classification and omit the regularization term, $\Omega(g)$. We define the loss function, $\mathcal{L}(f, \boldsymbol{\theta}, \pi_{\mathbf{x}, \mathbf{c}})$, as:

$$\mathcal{L} = \frac{1}{K} \sum_{k=1}^K (\operatorname{logit} p(Y = 1 | \mathbf{x}_k - \mathbf{x}, \mathbf{c}_k) - \operatorname{logit} p(Y = 1 | \mathbf{x}_k - \mathbf{x}, \boldsymbol{\theta}))^2, \quad (15)$$

where $(\mathbf{x}_k, \mathbf{c}_k) \sim \pi_{\mathbf{x}, \mathbf{c}}$ and $\pi_{\mathbf{x}, \mathbf{c}} := \pi_{\mathbf{x}} \pi_{\mathbf{c}}$ is a distribution concentrated around (\mathbf{x}, \mathbf{c}) . Without loss of generality, we also drop the bias terms in the linear models and assume that $\mathbf{a}(\mathbf{x}_k - \mathbf{x})$ are centered.

Proof of Theorem 1. The optimization problem (14) reduces to the least squares linear regression:

$$\hat{\boldsymbol{\theta}} = \operatorname{argmin}_{\boldsymbol{\theta}} \frac{1}{K} \sum_{k=1}^K (\operatorname{logit} p(Y = 1 | \mathbf{x}_k - \mathbf{x}, \mathbf{c}_k) - \mathbf{a}(\mathbf{x}_k - \mathbf{x})^\top \boldsymbol{\theta})^2 \quad (16)$$

We consider deterministic encoding, $p(\boldsymbol{\theta} | \mathbf{c}) := \delta(\boldsymbol{\theta}, \phi(\mathbf{c}))$, and hence $\operatorname{logit} p(Y = 1 | \mathbf{x}_k - \mathbf{x}, \mathbf{c}_k)$ takes the following form:

$$\operatorname{logit} p(Y = 1 | \mathbf{x}_k - \mathbf{x}, \mathbf{c}_k) = \operatorname{logit} p(Y = 1 | \mathbf{x}_k - \mathbf{x}, \boldsymbol{\theta} = \phi(\mathbf{c}_k)) = \mathbf{a}(\mathbf{x}_k - \mathbf{x})^\top \phi(\mathbf{c}_k) \quad (17)$$

To simplify the notation, we denote $\mathbf{a}_k := \mathbf{a}(\mathbf{x}_k - \mathbf{x})$, $\phi_k := \phi(\mathbf{c}_k)$, and $\phi := \phi(\mathbf{c})$. The solution of (16) now can be written in a closed form:

$$\hat{\boldsymbol{\theta}} = \left[\frac{1}{K} \sum_{k=1}^K \mathbf{a}_k \mathbf{a}_k^\top \right]^+ \left[\frac{1}{K} \sum_{k=1}^K \mathbf{a}_k \mathbf{a}_k^\top \phi_k \right] \quad (18)$$

Note that $\hat{\boldsymbol{\theta}}$ is a random variable since $(\mathbf{x}_k, \mathbf{c}_k)$ are randomly generated from $\pi_{\mathbf{x}, \mathbf{c}}$. To further simplify the notation, denote $M := \frac{1}{K} \sum_{k=1}^K \mathbf{a}_k \mathbf{a}_k^\top$. To get a concentration bound on $\|\hat{\boldsymbol{\theta}} - \boldsymbol{\theta}^*\|$, we will use the continuity of $\phi(\cdot)$ and $\mathbf{a}(\cdot)$, concentration properties of $\pi_{\mathbf{x}, \mathbf{c}}$ around (\mathbf{x}, \mathbf{c}) , and some elementary results from random matrix theory. To be more concrete, since we assumed that $\pi_{\mathbf{x}, \mathbf{c}}$ factorizes, we further let $\pi_{\mathbf{x}}$ and $\pi_{\mathbf{c}}$ concentrate such that $p_{\pi_{\mathbf{x}}}(\|\mathbf{x}' - \mathbf{x}\| > t) < \varepsilon_{\mathbf{x}}(t)$ and $p_{\pi_{\mathbf{c}}}(\|\mathbf{c}' - \mathbf{c}\| > t) < \varepsilon_{\mathbf{c}}(t)$, respectively, where $\varepsilon_{\mathbf{x}}(t)$ and $\varepsilon_{\mathbf{c}}(t)$ both go to 0 as $t \rightarrow \infty$, potentially at different rates.

First, we have the following bound from the convexity of the norm:

$$p\left(\|\hat{\boldsymbol{\theta}} - \boldsymbol{\theta}^*\| > t\right) = p\left(\left\| \frac{1}{K} \sum_{k=1}^K [M^+ \mathbf{a}_k \mathbf{a}_k^\top (\phi_k - \phi)] \right\| > t\right) \quad (19)$$

$$\leq p\left(\frac{1}{K} \sum_{k=1}^K \|M^+ \mathbf{a}_k \mathbf{a}_k^\top (\phi_k - \phi)\| > t\right) \quad (20)$$

¹⁰In case of logistic regression, $\mathbf{a}(\mathbf{x}) = [1, x_1, \dots, x_d]^\top$.

By making use of the inequality $\|Ax\| \leq \|A\|\|x\|$, where $\|A\|$ denotes the spectral norm of the matrix A , the L -Lipschitz property of $\phi(\mathbf{c})$, the C -Lipschitz property of $\mathbf{a}(\mathbf{x})$, and the concentration of \mathbf{x}_k around \mathbf{x} , we have

$$p\left(\|\hat{\boldsymbol{\theta}} - \boldsymbol{\theta}^*\| > t\right) \leq p\left(L\frac{1}{K}\sum_{k=1}^K\|M^+\mathbf{a}_k\mathbf{a}_k^\top\|\|\mathbf{c}_k - \mathbf{c}\| > t\right) \quad (21)$$

$$\leq p\left(CL\|M^+\|\frac{1}{K}\sum_{k=1}^K\|\mathbf{a}_k\mathbf{a}_k^\top\|\|\mathbf{c}_k - \mathbf{c}\| > t\right) \quad (22)$$

$$\leq p\left(\frac{CL}{\lambda_{\min}(M)}\frac{1}{K}\sum_{k=1}^K\|\mathbf{x}_k - \mathbf{x}\|\|\mathbf{c}_k - \mathbf{c}\| > t\right) \quad (23)$$

$$\leq p\left(\frac{CL\tau^2}{\lambda_{\min}(M)} > t\right) + p\left(\|\mathbf{x}_k - \mathbf{x}\|\|\mathbf{c}_k - \mathbf{c}\| > \tau^2\right) \quad (24)$$

$$\leq p\left(\lambda_{\min}(M/(C\tau)^2) < \frac{L}{C^2t}\right) + \varepsilon_{\mathbf{x}}(\tau) + \varepsilon_{\mathbf{c}}(\tau) \quad (25)$$

Note that we used the fact that the spectral norm of a rank-1 matrix, $\mathbf{a}(\mathbf{x}_k)\mathbf{a}(\mathbf{x}_k)^\top$, is simply the norm of $\mathbf{a}(\mathbf{x}_k)$, and the spectral norm of the pseudo-inverse of a matrix is equal to the inverse of the least non-zero singular value of the original matrix: $\|M^+\| \leq \lambda_{\max}(M^+) = \lambda_{\min}^{-1}(M)$.

Finally, we need a concentration bound on $\lambda_{\min}(M/(C\tau)^2)$ to complete the proof. Note that $\frac{M}{C^2\tau^2} = \frac{1}{K}\sum_{k=1}^K\left(\frac{\mathbf{a}_k}{C\tau}\right)\left(\frac{\mathbf{a}_k}{C\tau}\right)^\top$, where the norm of $\left(\frac{\mathbf{a}_k}{C\tau}\right)$ is bounded by 1. If we denote $\mu_{\min}(C\tau)$ the minimal eigenvalue of $\text{Cov}\left[\frac{\mathbf{a}_k}{C\tau}\right]$, we can write the matrix Chernoff inequality [3] as follows:

$$p\left(\lambda_{\min}(M/(C\tau)^2) < \alpha\right) \leq d \exp\{-KD(\alpha\|\mu_{\min}(C\tau))\}, \quad \alpha \in [0, \mu_{\min}(C\tau)],$$

where d is the dimension of \mathbf{a}_k , $\alpha := \frac{L}{C^2t}$, and $D(a\|b)$ denotes the binary information divergence:

$$D(a\|b) = a \log\left(\frac{a}{b}\right) + (1-a) \log\left(\frac{1-a}{1-b}\right).$$

The final concentration bound has the following form:

$$p\left(\|\hat{\boldsymbol{\theta}} - \boldsymbol{\theta}^*\| > t\right) \leq d \exp\left\{-KD\left(\frac{L}{C^2t}\|\mu_{\min}(C\tau)\right)\right\} + \varepsilon_{\mathbf{x}}(\tau) + \varepsilon_{\mathbf{c}}(\tau) \quad (26)$$

We see that as $\tau \rightarrow \infty$ and $t \rightarrow \infty$ all terms on the right hand side vanish, and hence $\hat{\boldsymbol{\theta}}$ concentrates around $\boldsymbol{\theta}^*$. Note that as long as $\mu_{\min}(C\tau)$ is far from 0, the first term can be made negligibly small by sampling more points around (\mathbf{x}, \mathbf{c}) . Finally, we set $\tau \equiv t$ and denote the right hand side by $\delta_{K,L,C}(t)$ that goes to 0 as $t \rightarrow \infty$ to recover the statement of the original theorem. \square

Remark 3. We have shown that $\hat{\boldsymbol{\theta}}$ concentrates around $\boldsymbol{\theta}^*$ under mild conditions. With more assumptions on the sampling distribution, $\pi_{\mathbf{x},\mathbf{c}}$, (e.g., sub-gaussian) one could derive precise convergence rates. Note that we are in total control of any assumptions we put on $\pi_{\mathbf{x},\mathbf{c}}$ since precisely that distribution is used for sampling. This is a major difference between the local approximation setup here and the setup of linear regression with random design; in the latter case, we have no control over the distribution of the design matrix, and any assumptions we make could potentially be unrealistic.

Remark 4. Note that concentration analysis of a more general case when the loss \mathcal{L} is a general convex function and $\Omega(g)$ is a decomposable regularizer could be done by using results from the M -estimation theory [4], but would be much more involved and unnecessary for our purposes.

C Learning and Inference in the Contextual Mixture of Experts

As noted in the main text, to make a prediction, MoE uses each of the K experts where the predictive distribution is computed as follows:

$$p_{\mathbf{w},\mathbf{D}}(\mathbf{Y} \mid \mathbf{X}, \mathbf{C}) = \sum_{k=1}^K p_{\mathbf{w}}(k \mid \mathbf{C}) p(\mathbf{Y} \mid \mathbf{X}, \boldsymbol{\theta}_k). \quad (27)$$

Since each expert contributes to the predictive probability, we can explain a prediction, \hat{y} , for the instance (\mathbf{x}, \mathbf{c}) in terms of the posterior weights assigned to each expert model:

$$p_{\mathbf{w}}(k | \hat{y}, \mathbf{x}, \mathbf{c}) = \frac{p_{\mathbf{w}}(\hat{y}, k | \mathbf{x}, \mathbf{c})}{p_{\mathbf{w}}(\hat{y} | \mathbf{x}, \mathbf{c})} = \frac{p(\hat{y} | \mathbf{x}, \boldsymbol{\theta}_k) p_{\mathbf{w}}(k | \mathbf{c})}{\sum_{k=1}^K p_{\mathbf{w}}(k | \mathbf{c}) p(\hat{y} | \mathbf{x}, \boldsymbol{\theta}_k)} \quad (28)$$

If the $p(k | \hat{y}, \mathbf{x}, \mathbf{c})$ assigns very high weight to a single expert, we can treat that expert model as an explanation. Note that however, in general, this may not be the case and posterior weights could be quite spread out (especially, if the number of experts is small and the class of expert models, $p(\mathbf{Y} | \mathbf{X}, \boldsymbol{\theta})$, is too simple and limited). Therefore, there may not exist an equivalent local explanation in the class of expert models that would faithfully approximate the decision boundary.

To learn contextual MoE, we can either directly optimize the conditional log-likelihood, which is non-convex yet tractable, or use expectation maximization (EM) procedure. For the latter, we write the log likelihood in the following form:

$$\log p(\mathbf{y} | \mathbf{x}, \mathbf{c}) = \sum_{k=1}^K q(k) \log p(\mathbf{y} | \mathbf{x}, \mathbf{c}) \quad (29)$$

$$= \sum_{k=1}^K q(k) \log \frac{p(\mathbf{y} | \mathbf{x}, \boldsymbol{\theta}_k) p_{\mathbf{w}}(k | \mathbf{c}) q(k)}{p_{\mathbf{w}}(k | \mathbf{y}, \mathbf{x}, \mathbf{c}) q(k)} \quad (30)$$

$$= \sum_{k=1}^K q(k) \log \frac{p(\mathbf{y} | \mathbf{x}, \boldsymbol{\theta}_k) p_{\mathbf{w}}(k | \mathbf{c})}{q(k)} + \text{KL}(q(k) \| p_{\mathbf{w}}(k | \mathbf{y}, \mathbf{x}, \mathbf{c})) \quad (31)$$

At each iteration, we do two steps:

(E-step) Compute posteriors for each data instance, $q_i(k) = p_{\mathbf{w}}(k | \mathbf{y}_i, \mathbf{x}_i, \mathbf{c}_i)$.

(M-step) Optimize $Q(\mathbf{w}) = \sum_{k=1}^K q(k) \log p(\mathbf{y} | \mathbf{x}, \boldsymbol{\theta}_k) p_{\mathbf{w}}(k | \mathbf{c})$.

It is well known that this iterative procedure is guaranteed to converge to a local optimum.

D Contextual Variational Autoencoders

We can express the evidence for contextual variational autoencoders as follows:

$$\begin{aligned} \log p(\mathbf{Y}, \mathbf{C} | \mathbf{X}) &= \int q_{\mathbf{w}}(\boldsymbol{\theta} | \mathbf{C}) \log p(\mathbf{Y}, \mathbf{C} | \mathbf{X}) d\boldsymbol{\theta} \\ &= \int q_{\mathbf{w}}(\boldsymbol{\theta} | \mathbf{C}) \log \frac{p(\mathbf{Y} | \mathbf{X}, \boldsymbol{\theta}) p_{\mathbf{u}}(\mathbf{C} | \boldsymbol{\theta}) p(\boldsymbol{\theta})}{p_{\mathbf{u}}(\boldsymbol{\theta} | \mathbf{Y}, \mathbf{X}, \mathbf{C})} d\boldsymbol{\theta} \\ &= \int q_{\mathbf{w}}(\boldsymbol{\theta} | \mathbf{C}) \log \frac{p(\mathbf{Y} | \mathbf{X}, \boldsymbol{\theta}) p_{\mathbf{u}}(\mathbf{C} | \boldsymbol{\theta}) p(\boldsymbol{\theta})}{q_{\mathbf{w}}(\boldsymbol{\theta} | \mathbf{C})} d\boldsymbol{\theta} + \text{KL}(q_{\mathbf{w}}(\boldsymbol{\theta} | \mathbf{C}) \| p_{\mathbf{u}}(\boldsymbol{\theta} | \mathbf{Y}, \mathbf{X}, \mathbf{C})) \\ &\geq \mathcal{L}(\mathbf{w}, \mathbf{u}; \mathbf{Y}, \mathbf{X}, \mathbf{C}), \end{aligned} \quad (32)$$

where $\mathcal{L}(\mathbf{w}, \mathbf{u}; \mathbf{Y}, \mathbf{X}, \mathbf{C})$ is the evidence lower bound (ELBO):

$$\begin{aligned} \mathcal{L}(\mathbf{w}, \mathbf{u}; \mathbf{Y}, \mathbf{X}, \mathbf{C}) &= \mathbb{E}_{q_{\mathbf{w}}} \left[\log \frac{p(\mathbf{Y} | \mathbf{X}, \boldsymbol{\theta}) p_{\mathbf{u}}(\mathbf{C} | \boldsymbol{\theta}) p(\boldsymbol{\theta})}{q_{\mathbf{w}}(\boldsymbol{\theta} | \mathbf{C})} \right] \\ &= \mathbb{E}_{q_{\mathbf{w}}} [\log p(\mathbf{Y} | \mathbf{X}, \boldsymbol{\theta})] + \mathbb{E}_{q_{\mathbf{w}}} [\log p_{\mathbf{u}}(\mathbf{C} | \boldsymbol{\theta})] - \text{KL}(q(\boldsymbol{\theta} | \mathbf{C}) \| p(\boldsymbol{\theta})) \end{aligned} \quad (33)$$

We notice that the ELBO consists of three terms:

- (1) the expected conditional likelihood of the explanation, $\mathbb{E}_{q_{\mathbf{w}}} [\log p(\mathbf{Y} | \mathbf{X}, \boldsymbol{\theta})]$,
- (2) the expected context reconstruction error, $\mathbb{E}_{q_{\mathbf{w}}} [\log p_{\mathbf{u}}(\mathbf{C} | \boldsymbol{\theta})]$, and
- (3) the KL-based regularization term, $-\text{KL}(q(\boldsymbol{\theta} | \mathbf{C}) \| p(\boldsymbol{\theta}))$.

We can optimize the ELBO using first-order methods by estimating the gradients via Monte Carlo sampling with reparametrization. When the encoder has a classical form of a Gaussian distribution (or any other location-scale type of distribution), $q_{\mathbf{w}}(\boldsymbol{\theta} | \mathbf{C}) = \mathcal{N}(\boldsymbol{\theta}; \boldsymbol{\mu}_{\mathbf{w}}(\mathbf{C}), \text{diag}(\boldsymbol{\sigma}_{\mathbf{w}}(\mathbf{C})))$, reparametrization of the samples is straightforward [5].

In our experiments, we mainly consider encoders that output probability distributions over a simplex spanned by a dictionary, \mathbf{D} , which turned out to have better performance and faster convergence. In particular, sampling from the encoder is as follows:

$$\begin{aligned} \mathbf{z} &\sim \mathcal{N}(\boldsymbol{\theta}; \boldsymbol{\mu}_{\mathbf{w}}(\mathbf{C}), \text{diag}(\boldsymbol{\sigma}_{\mathbf{w}}(\mathbf{C}))), \\ \gamma_0 &= \frac{1}{1 + \sum_{j=1}^K e^{z_j}}, \gamma_i = \frac{e^{z_i}}{1 + \sum_{j=1}^K e^{z_j}}, i = 1, \dots, K, \\ \boldsymbol{\theta} &= \mathbf{D} \cdot \boldsymbol{\gamma} \end{aligned} \quad (34)$$

The samples, $\boldsymbol{\theta}$, will be logistic normal distributed and are easy to be re-parametrized. For prior, we use the Dirichlet distribution over $\boldsymbol{\gamma}$ with the parameter vector $\boldsymbol{\alpha}$. In that case, the stochastic estimate of the KL-based regularization term has the following form:

$$-\text{KL}(q(\boldsymbol{\gamma} | \mathbf{C}) \| p(\boldsymbol{\gamma})) \simeq \frac{1}{L} \sum_{l=1}^L \log \mathcal{N} \left(\log \left(\frac{\boldsymbol{\gamma}_{-0}^{(l)}}{\boldsymbol{\gamma}_0^{(l)}} \right); \boldsymbol{\mu}_{\mathbf{w}}(\mathbf{C}), \text{diag}(\boldsymbol{\sigma}_{\mathbf{w}}(\mathbf{C})) \right) - \boldsymbol{\alpha}^\top \log(\boldsymbol{\gamma}^{(l)}), \quad (35)$$

where $\boldsymbol{\gamma}_{-0}^{(l)}$ is a parameter vector without the first element, and l indexes samples taken from the encoder, $p(\boldsymbol{\gamma} | \mathbf{C})$. In practice, we use $L = 1$.

E Contextual Conditional Random Fields for Survival Analysis

In case of the structured outputs, $p(\mathbf{Y} | \mathbf{X}, \boldsymbol{\theta})$ could be represented by a CRF of an arbitrary structure. In general, prediction would require inference; when the inference can be exact (e.g., for linearly structured CRFs we can use the forward-backward algorithm), it can be incorporated as a part of the computation graph¹¹.

Chun-Nam et al. [6] show that linear chain CRF can naturally account for censored data. When we have hard constraints on some transitions (as described in the main text), it turns out that inference becomes straightforward and can be done in linear time, and the censored (unobserved) events can be marginalized out also in linear time. This allows us to write the likelihood of an uncensored event that happened at time t_j as:

$$p(T = t_j | \mathbf{x}, \boldsymbol{\Theta}) = \exp \left\{ \sum_{i=j}^m \mathbf{x}^\top \boldsymbol{\theta}_i \right\} / \sum_{k=0}^m \exp \left\{ \sum_{i=k+1}^m \mathbf{x}^\top \boldsymbol{\theta}_i \right\}, \quad (36)$$

and the likelihood of an event censored at time t_j in the following form:

$$p(T \geq t_j | \mathbf{x}, \boldsymbol{\Theta}) = \sum_{k=j}^m \exp \left\{ \sum_{i=k+1}^m \mathbf{x}^\top \boldsymbol{\theta}_i \right\} / \sum_{k=0}^m \exp \left\{ \sum_{i=k+1}^m \mathbf{x}^\top \boldsymbol{\theta}_i \right\}. \quad (37)$$

The joint log-likelihood will consist of two parts: (a) the sum over the non-censored instances, for which we compute $\log p(T = t_j | \mathbf{x}, \boldsymbol{\Theta})$, and (b) sum over the censored instances, for which we use $\log p(T \geq t_j | \mathbf{x}, \boldsymbol{\Theta})$ computed as in (37). We optimize the objective using stochastic gradient method, and hence for each mini-batch, depending on which instances are censored and which are non-censored, we construct the objective function accordingly. To implement this in TensorFlow, we define the objective using the standard control flow primitives that select either (36) or (37) for each sample in the mini-batch based on the censorship indicator.

¹¹If $p(\mathbf{Y} | \mathbf{X}, \boldsymbol{\theta})$ requires iterative approximate inference, one could still backpropagate through the unfolded computation of the approximation procedure.

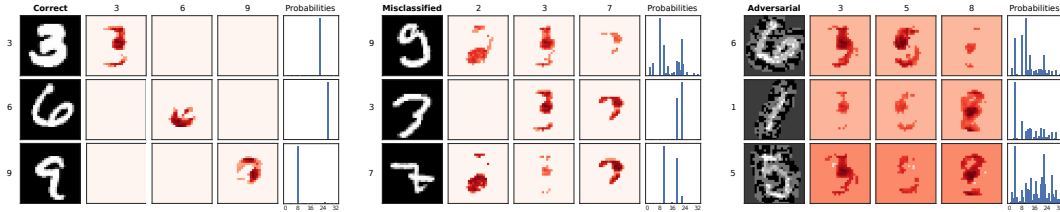


Figure 6: Visualization of the top 3 prediction rationalizations provided by the $\text{CIM}_{\text{pxl}}^{\text{CNN}}$ model for correctly classified (left), misclassified (middle), and adversarial (right) digits. Adversarial examples were generated using the fast gradient sign method (FGSM) [9].

F Addendum to Experiments

This section provides details on the experimental setups including architectures, training protocols and procedures, etc. Additionally, we include complete dictionary visualizations learned by CENs.

F.1 Additional Details on the Datasets and Experiment Setups

MNIST. We used the classical split of the dataset into 50k training, 10k validation, and 10k testing points. All models were trained for 100 epochs using the Adam optimizer with the learning rate of 10^{-3} . No data augmentation was used in any of our experiments. HOG representations were computed using 3×3 blocks.

CIFAR10. For this set of experiments, we followed the setup given Zagoruyko [7], reimplemented in Keras with TensorFlow backend. The input images were global contrast normalized (a.k.a. GCN whitened) while the rescaled image representations were simply standardized. Again, HOG representations were computed using 3×3 blocks. No data augmentation was used in our experiments.

IMDB. We considered the labeled part of the data only (50k reviews total). The data were split into 20k train, 5k validation, and 25k test points. All models were trained with the Adam optimizers with 10^{-2} learning rate. The models were initialized randomly; no pre-training or any other unsupervised/semi-supervised technique was used.

Satellite. As described in the main text, we used a pre-trained VGG-16 network¹² to extract features from the satellite imagery. Further, we added one fully connected layer network with 128 hidden units used as the context encoder. For the VCEN model, we used dictionary-based encoding with Dirichlet prior and logistic normal distribution as the output of the inference network. For the decoder, we used an MLP of the same architecture as the encoder network. All models were trained with Adam optimizer with 0.05 learning rate. The results were obtained by 5-fold cross-validation.

Medical data. We have used minimal pre-processing of both SUPPORT2 and PhysioNet datasets limited to standardization and missing-value filling. We found that denoting missing values with negative entries (-1) often led a slightly improved performance compared to any other NA-filling techniques. PhysioNet time series data was irregularly sampled across the time, so we had to resample temporal sequences at regular intervals of 30 min (consequently, this has created quite a few missing values for some of the measurements). All models were trained using Adam optimizer with 10^{-2} learning rate.

F.2 Model Architectures

Architectures of the model used in our experiments are summarized in Tables 4, 5, 6.

F.3 Dictionaries Learned by CENs

We visualize the full dictionaries learned by CENs on MNIST, IMDB, and Satellite tasks (see Figures 6, 7, 9, 8, 10a) and additional correlation plots between the selected models and the survey variable values (Figure 10b).

¹²The model was taken from <https://github.com/nealjean/predicting-poverty>.

Table 4: Top-performing architectures used in our experiments on MNIST and IMDB datasets.

(a) MNIST				(b) IMDB				
Convolutional Encoder		Contextual Explanations		Sequential Encoder		Contextual Explanations		
Convolutional Block	layer	Conv2D	model	Logistic reg.	layer	Embedding	model	Logistic reg.
	# filters	32	features	HOG (3, 3)	vocabulary	20k	features	BoW
	kernel size	3×3	# of features	729	dimension	1024	# of features	20k
	strides	1×1	standardized	Yes	layer	LSTM	Dictionary	32
	padding	valid	dictionary	256			bidirectional	Yes
	activation	ReLU	l_1 penalty	$5 \cdot 10^{-5}$	units	256	l_2 penalty	$1 \cdot 10^{-6}$
			l_2 penalty	$1 \cdot 10^{-6}$	max length	200	model	Logistic reg.
	layer	Conv2D	model	Logistic reg.	dropout	0.25	features	Topics
	# filters	32	features	Pixels (20, 20)	rec. dropout	0.25	# of features	50
	kernel size	3×3	# of features	400	layer	MaxPool1D	Dictionary	16
strides	1×1	standardized	Yes	# params	23.1M	l_1 penalty	$1 \cdot 10^{-6}$	
padding	valid	dictionary	64			l_2 penalty	$1 \cdot 10^{-8}$	
activation	ReLU	l_1 penalty	$5 \cdot 10^{-5}$	Contextual VAE				
		l_2 penalty	$1 \cdot 10^{-6}$	Prior		Dir(0.1)		
layer	MaxPool2D	prior	Dir(0.2)	Sampler		LogisticNormal		
pooling size	2×2	sampler	LogisticNormal					
dropout	0.25							
		Contextual VAE						
layer	Dense							
units	128							
dropout	0.50							
# of blocks	1							
# params	1.2M							

Table 5: Top-performing architectures used in our experiments on CIFAR10 and Satellite datasets. VGG-16 architecture for CIFAR10 was taken from https://github.com/szagoruyko/cifar_torch but implemented in Keras with TensorFlow backend. Weights of the pre-trained VGG-F model for the Satellite experiments were taken from <https://github.com/nealjean/predicting-poverty>.

(a) CIFAR10				(b) Satellite					
Convolutional Encoder		Contextual Explanations		Convolutional Encoder		Contextual Explanations			
VGG-16	model	VGG-16	model	Logistic reg.	VGG-F	model	VGG-F	model	Logistic reg.
	pretrained	No	features	HOG (3, 3)		pretrained	Yes	features	Survey
	frozen weights	No	# of features	1024		frozen weights	Yes	# of features	64
	reference	[7]	dictionary	16		reference	[8]	dictionary	16
		l_1 penalty	$1 \cdot 10^{-5}$			l_1 penalty	$1 \cdot 10^{-3}$		
		l_2 penalty	$1 \cdot 10^{-6}$			l_2 penalty	$1 \cdot 10^{-4}$		
		Contextual VAE				Contextual VAE			
MLP	layer	Dense	prior	Dir(0.2)	MLP	layer	Dense	prior	Dir(0.2)
	pretrained	No	sampler	LogisticNormal		pretrained	No	sampler	LogisticNormal
	frozen weights	No				frozen weights	No		
	units	16				units	128		
dropout	0.25			dropout	0.25				
activation	ReLU			activation	ReLU				
# params	20.0M			# trainable params					

Table 6: Top-performing architectures used in our experiments on SUPPORT2 and PhysioNet 2012 datasets.

(a) SUPPORT2				(b) PhysioNet Challenge 2012					
MLP Encoder		Contextual Explanations		Sequential Encoder		Contextual Explanations			
MLP	layer	Dense	model	Linear CRF	LSTM	layer	LSTM	model	Linear CRF
	pretrained	No	features	Measurements		bidirectional	No	features	Statistics
	frozen weights	No	# of features	51		units	32	# of features	111
	units	64	dictionary	16		max length	150	dictionary	16
	dropout	0.50	l_1 penalty	$1 \cdot 10^{-3}$		dropout	0.25	l_1 penalty	$1 \cdot 10^{-3}$
	activation	ReLU	l_2 penalty	$1 \cdot 10^{-4}$		rec. dropout	0.25	l_2 penalty	$1 \cdot 10^{-4}$



Figure 7: Visualization of the model dictionary learned by CEN on MNIST. Each row corresponds to a dictionary element, and each column corresponds to the weights of the model voting for each class of digits. Images visualize the weights of the models. Red corresponds to high positive values, dark gray to high negative values, and white to values that are close to 0.

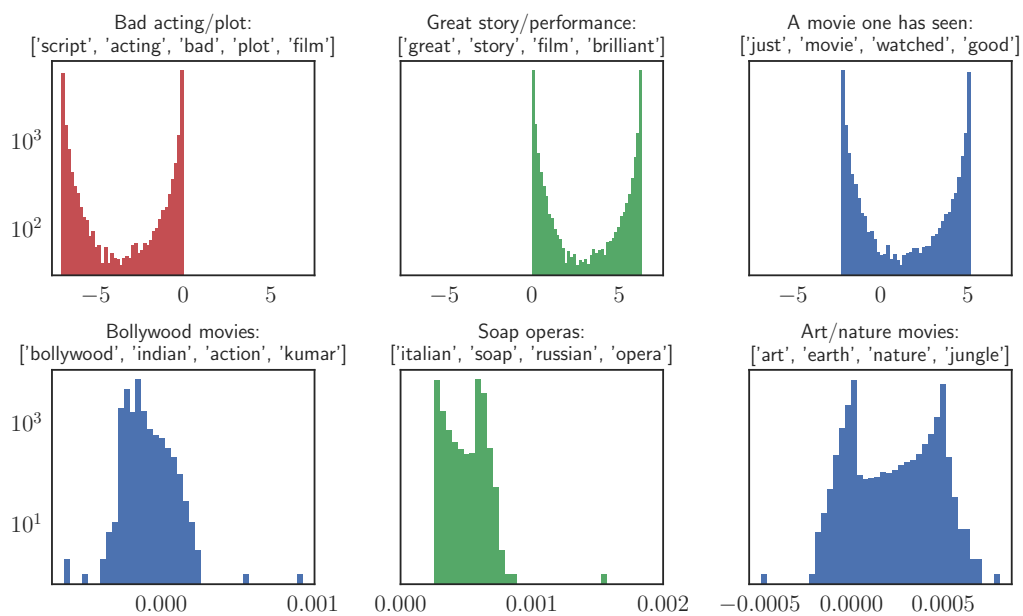
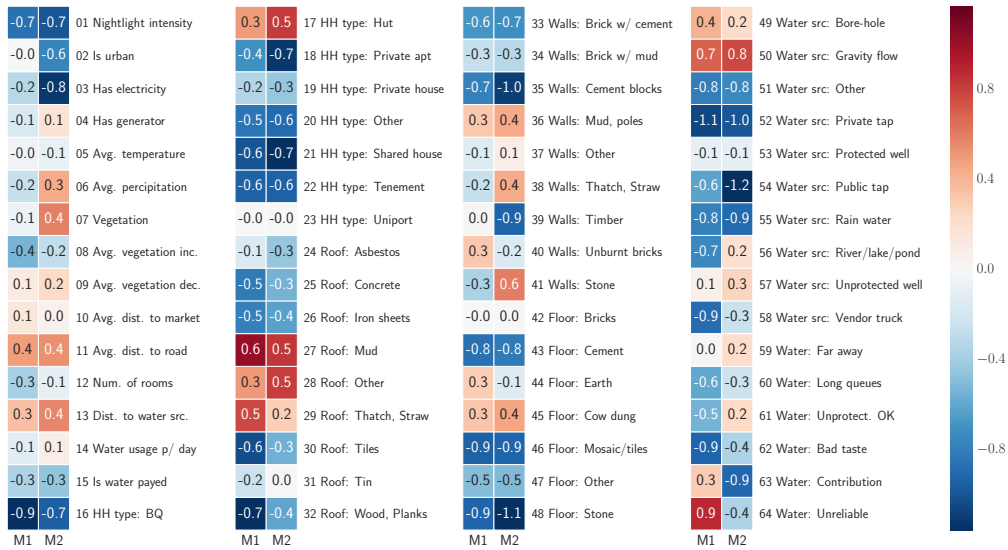


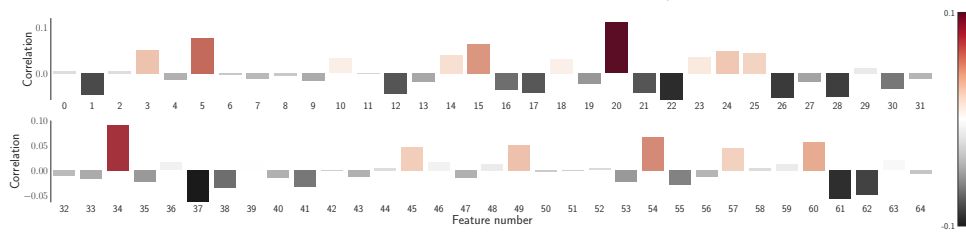
Figure 8: Histograms of test weights assigned by CEN to 6 topics: Acting- and plot-related topics (upper charts), genre topics (bottom charts). Note that acting-related topics are often bi-modal, i.e., contributing either positive, negative, or zero weight to the sentiment prediction in different contexts. Genre topics almost always have negligible contributions. This allows us to conclude that the learned model does not have any particular biases towards or against any a given genre.

	1	2	3	4	5	6	7	8	9	10	11	12	13	14	15	16
[students, version, branagh, high, shakespeare, school, play]	1	0.0	0.0	0.0	-0.2	-0.2	0.0	0.3	-0.2	-0.2	0.0	0.0	-0.2	0.0	0.0	0.0
[jackie, chinese, japanese, dog, just, action, scene]	2	-0.3	0.2	0.0	0.1	0.3	0.0	0.0	0.0	-0.3	0.2	0.0	0.2	0.2	0.0	0.1
[don, man, t. stewart, u. western, s]	3	0.1	0.0	-0.2	-0.2	0.3	0.0	0.2	-0.2	-0.1	0.0	0.0	0.1	0.1	0.0	0.3
[luke, adaptation, version, jane, read, novel, book]	4	0.0	0.0	0.3	-0.1	-0.2	0.0	0.2	-0.2	-0.2	-0.2	0.0	0.0	0.1	0.0	0.2
[elvis, brando, stephen, jackson, chris, king, michael]	5	0.0	0.1	0.0	0.0	0.0	0.0	0.2	-0.2	0.2	-0.2	-0.2	0.2	0.0	0.0	0.2
[budget, scary, zombie, effects, film, gore, horror]	6	0.0	0.0	0.0	-0.1	-0.2	0.3	-0.2	-0.2	-0.2	0.3	-0.3	0.2	0.3	0.0	0.1
[oh, loved, li, totally, oliver, wow, !]	7	0.0	0.1	0.0	-0.2	0.0	0.2	0.0	0.3	0.2	0.1	0.2	-0.3	-0.2	0.0	0.1
[cole, british, virus, time, bush, irish, james]	8	-0.1	0.0	0.2	0.0	0.0	-0.2	-0.2	0.0	-0.2	0.2	0.0	0.0	-0.2	0.1	-0.1
[film, wellies, noir, city, new, joe, york]	9	0.1	0.0	-0.2	-0.3	-0.1	0.2	0.1	0.2	-0.1	-0.2	0.3	-0.2	0.0	0.0	0.2
[kate, caine, performance, alan, cast, role, peter]	10	0.0	0.1	0.2	-0.2	-0.2	0.1	0.0	-0.2	-0.1	-0.2	0.3	-0.2	0.1	0.1	0.0
[script, characters, just, acting, bad, plot, film]	11	-0.5	-0.6	0.0	0.0	-0.2	0.0	-0.1	-0.4	0.0	0.0	-0.4	-0.4	0.2	-0.5	0.2
[camp, arts, martial, fight, action, lee, game]	12	0.0	0.2	0.0	0.0	0.3	-0.2	-0.2	0.0	-0.2	0.2	0.3	-0.2	-0.3	0.1	0.2
[kid, child, little, disney, family, children, kids]	13	0.0	0.0	0.0	0.1	0.3	0.0	0.0	-0.1	-0.2	0.2	-0.2	0.1	-0.2	0.0	0.1
[robert, bank, roy, pacino, rob, mary, al]	14	0.0	-0.1	0.2	0.1	0.0	0.0	0.3	0.3	0.2	-0.2	0.0	0.0	0.0	0.0	0.0
[rose, hardy, sutherland, titanic, steve, jack, george]	15	-0.1	0.2	0.2	0.0	0.1	0.0	-0.4	0.0	0.1	0.2	0.0	-0.2	0.3	0.0	-0.1
[really, don't, ?, just, like, bad, movie]	16	-0.7	-0.5	0.2	-0.2	-0.2	-0.4	-0.3	-0.3	0.0	0.0	-0.3	0.0	0.1	-0.6	0.2
[films, beautiful, love, characters, great, story, film]	17	0.4	0.3	-0.2	-0.2	0.0	-0.1	0.3	0.0	-0.2	0.0	0.0	0.3	0.1	0.6	0.0
[man, racist, like, film, american, white, black]	18	-0.2	0.0	0.0	0.2	-0.2	0.0	0.0	-0.2	-0.2	-0.3	-0.2	0.0	0.1	0.0	-0.1
[great, soundtrack, band, songs, song, rock, music]	19	0.1	0.0	0.0	-0.2	0.2	-0.3	0.0	0.0	-0.2	0.3	0.0	0.2	-0.1	0.1	0.0
[clark, street, africa, nightmare, south, freddy, superman]	20	0.0	0.0	-0.2	0.0	0.3	0.0	0.0	0.3	0.0	0.2	0.0	-0.2	-0.2	0.0	-0.2
[john, tv, sam, candy, murphy, eddie, night]	21	-0.2	0.0	0.0	0.3	0.0	0.0	0.2	0.0	-0.1	0.0	-0.2	0.0	0.3	-0.1	-0.2
[sky, ship, trek, richard, captain, star, scott]	22	0.1	0.0	0.2	0.2	0.0	0.1	0.0	0.0	-0.2	0.0	0.0	0.2	0.0	0.0	-0.2
[maria, new, london, mr, young, movie, ford]	23	0.0	0.2	0.2	-0.2	-0.1	0.0	0.3	0.3	0.3	0.0	0.2	0.2	0.0	0.0	0.0
[music, astaire, rogers, ted, fred, dancing, dance]	24	0.0	0.0	-0.1	0.2	0.0	0.1	0.0	-0.2	0.2	0.1	0.0	-0.1	0.2	0.0	-0.1
[think, just, really, good, like, films, film]	25	0.0	0.0	-0.1	0.2	0.2	0.4	-0.1	0.0	0.3	-0.2	0.3	-0.1	-0.2	0.1	0.0
[seagal, steven, bollywood, jeff, sandler, adam, indian]	26	0.0	0.0	0.1	0.0	0.0	0.0	0.0	0.0	-0.3	0.0	0.0	0.3	0.1	0.0	0.3
[human, like, world, way, film, life, people]	27	0.2	0.3	-0.2	0.0	-0.2	0.3	0.1	0.0	0.3	-0.3	0.3	0.2	0.0	0.1	0.0
[mr, hudson, emma, italian, soap, russian, opera]	28	0.0	0.0	-0.1	0.0	0.0	0.1	0.2	0.0	0.2	-0.1	0.0	0.1	-0.1	-0.1	-0.3
[man, released, video, release, version, film, dvd]	29	0.1	0.1	0.3	0.2	0.3	0.0	0.3	-0.2	0.0	0.3	0.1	0.3	0.0	0.1	0.2
[scene, women, sexual, scenes, violence, nudity, sex]	30	0.0	0.0	0.0	0.0	-0.2	-0.1	0.0	0.0	0.0	0.0	0.2	0.0	0.1	0.0	-0.1
[charlie, batman, animated, cartoon, original, animation, like]	31	0.1	0.1	0.1	-0.3	-0.1	0.0	-0.2	0.0	0.0	-0.2	0.0	-0.1	0.3	0.0	0.1
[baseball, team, williams, santa, ben, match, christmas]	32	-0.1	0.0	0.0	0.1	-0.2	0.2	0.0	0.0	0.3	0.0	0.2	0.0	0.3	0.1	-0.1
[football, city, segment, world, paris, men, women]	33	0.0	0.0	0.0	0.2	-0.1	0.3	0.3	-0.2	-0.3	0.0	0.0	0.2	0.0	0.0	-0.3
[watch, movies, really, good, like, just, movie]	34	0.0	0.3	-0.1	0.0	-0.2	0.0	0.3	0.3	0.0	0.0	0.0	-0.2	-0.2	0.1	-0.3
[beautiful, earth, time, film, art, french, tarzan]	35	0.0	0.1	-0.2	0.2	0.0	0.2	0.2	0.0	-0.1	0.2	0.2	0.3	0.0	0.2	0.3
[wife, gets, murder, horror, man, house, killer]	36	0.1	-0.2	-0.3	0.0	-0.3	0.0	0.0	0.0	-0.3	0.0	-0.2	0.2	0.0	0.1	-0.2
[question, think, don't, does, know, did, ?]	37	-0.1	0.0	0.2	-0.2	-0.2	0.0	0.2	-0.3	0.1	-0.3	0.2	0.2	-0.1	0.0	-0.2
[man, young, woman, father, family, life, love]	38	0.0	0.2	0.0	0.3	-0.1	0.1	0.0	0.0	0.1	0.0	0.3	0.0	0.3	0.0	-0.2
[school, religious, jesus, movie, church, christian, god]	39	0.0	-0.1	-0.2	-0.1	0.0	0.0	-0.2	0.1	0.0	0.0	-0.2	-0.3	-0.1	0.0	-0.2
[won, award, actor, role, oscar, performance, best]	40	0.0	0.0	0.1	0.0	0.0	-0.2	0.1	0.0	0.3	0.0	0.0	0.2	-0.3	0.1	0.2
[time, shows, season, episodes, tv, episode, series]	41	0.2	0.1	-0.1	0.0	-0.2	-0.2	-0.2	0.2	0.2	0.0	0.2	0.1	-0.3	0.1	0.0
[laughs, hilarious, laugh, jokes, humor, funny, comedy]	42	0.2	0.2	0.0	0.0	0.2	0.0	-0.1	-0.1	0.0	0.1	0.0	-0.2	0.2	0.1	0.0
[best, great, role, hollywood, arthur, kelly, musical]	43	-0.1	0.2	-0.1	0.0	-0.3	0.1	-0.3	0.1	0.0	0.2	-0.2	-0.2	-0.2	0.1	0.2
[school, girl, teenage, family, dad, house, girls]	44	0.1	0.0	0.2	0.0	0.2	0.0	0.2	-0.3	0.2	0.2	-0.2	-0.2	0.1	0.1	0.2
[flynn, detective, jim, murder, anne, marie, powell]	45	0.1	0.0	-0.2	0.2	0.0	0.2	0.0	-0.1	0.2	0.0	0.2	0.1	-0.1	0.0	0.2
[elvira, money, j. cast, danny, alex, tony]	46	0.2	0.0	0.0	-0.1	-0.2	0.0	0.2	0.2	0.0	0.2	0.2	0.2	-0.1	0.0	0.3
[van, nancy, check, julia, drew, vampires, vampire]	47	0.0	0.1	0.2	0.3	0.3	-0.2	0.0	0.0	0.0	0.2	-0.1	-0.2	-0.2	-0.1	-0.3
[action, really, story, like, character, good, movie]	48	0.0	0.0	0.2	0.2	0.0	-0.2	0.0	0.0	0.1	0.1	0.0	-0.2	0.0	0.1	-0.2
[director, page, shot, new, festival, documentary, film]	49	0.0	0.2	0.2	0.1	-0.2	0.0	0.0	0.2	-0.2	0.0	-0.2	0.3	0.2	0.0	0.0
[japanese, military, soldiers, history, world, american, war]	50	-0.1	0.0	0.0	0.0	0.0	0.0	0.2	0.0	0.2	-0.1	0.0	0.0	-0.3	0.1	0.0

Figure 9: The full dictionary learned by CEN_{tpc} model: rows correspond to topics and columns correspond to dictionary atoms. Very small values were thresholded for visualization clarity. Different atoms capture different prediction patterns; for example, atom 5 assigns a highly positive weight to the [kid, child, disney, family] topic and down-weights [sexual, violence, nudity, sex], while atom 11 acts in an opposite manner. Given the context of the review, CEN combines just a few atoms to make a prediction.



(a) Full visualization of models M1 and M2 learned by CEN on Satellite data.



(b) Correlation between the selected model and the value of a particular survey variable.

Figure 10: Additional visualizations for CENs trained on the Satellite data.

References

- [1] Wenxin Jiang and Martin A Tanner. “Hierarchical mixtures-of-experts for exponential family regression models: approximation and maximum likelihood estimation”. In: *Annals of Statistics* (1999), pp. 987–1011.
- [2] Marco Tulio Ribeiro, Sameer Singh, and Carlos Guestrin. “Why Should I Trust You?: Explaining the Predictions of Any Classifier”. In: *Proceedings of the 22nd ACM SIGKDD International Conference on Knowledge Discovery and Data Mining*. ACM. 2016, pp. 1135–1144.
- [3] Joel A Tropp. “User-friendly tail bounds for sums of random matrices”. In: *Foundations of computational mathematics* 12.4 (2012), pp. 389–434.
- [4] Sahand Negahban, Bin Yu, Martin J Wainwright, and Pradeep K Ravikumar. “A unified framework for high-dimensional analysis of m -estimators with decomposable regularizers”. In: *Advances in Neural Information Processing Systems*. 2009, pp. 1348–1356.
- [5] Diederik P Kingma and Max Welling. “Auto-encoding variational bayes”. In: *arXiv preprint arXiv:1312.6114* (2013).
- [6] J Yu Chun-Nam, Russell Greiner, Hsiu-Chin Lin, and Vickie Baracos. “Learning patient-specific cancer survival distributions as a sequence of dependent regressors”. In: *Advances in Neural Information Processing Systems*. 2011, pp. 1845–1853.
- [7] Sergey Zagoruyko. *92.45% on CIFAR-10 in Torch*. <http://torch.ch/blog/2015/07/30/cifar.html>. Blog. 2015.
- [8] Neal Jean, Marshall Burke, Michael Xie, W Matthew Davis, David B Lobell, and Stefano Ermon. “Combining satellite imagery and machine learning to predict poverty”. In: *Science* 353.6301 (2016), pp. 790–794.
- [9] Nicolas Papernot, Patrick McDaniel, Ian Goodfellow, Somesh Jha, Z Berkay Celik, and Ananthram Swami. “Practical Black-Box Attacks against Deep Learning Systems using Adversarial Examples”. In: *arXiv preprint arXiv:1602.02697* (2016).